# INFORMATION TO USERS

This manuscript has been reproduced from the microfilm master. UMI films the text directly from the original or copy submitted. Thus, some thesis and dissertation copies are in typewriter face, while others may be from any type of computer printer.

**The quality of this reproduction is dependent upon the quality of the copy submitted.** Broken or indistinct print, colored or poor quality illustrations and photographs, print bleedthrough, substandard margins, and improper alignment can adversely affect reproduction.

In the unlikely event that the author did not send UMI a complete manuscript and there are missing pages, these will be noted. Also, if unauthorized copyright material had to be removed, a note will indicate the deletion.

Oversize materials (e.g., maps, drawings, charts) are reproduced by sectioning the original, beginning at the upper left-hand corner and continuing from left to right in equal sections with small overlaps. Each original is also photographed in one exposure and is included in reduced form at the back of the book.

Photographs included in the original manuscript have been reproduced xerographically in this copy. Higher quality 6" x 9" black and white photographic prints are available for any photographs or illustrations appearing in this copy for an additional charge. Contact UMI directly to order.
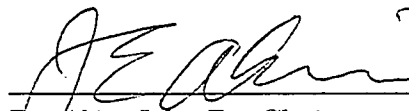
# UMI

RICE UNIVERSITY

# VIBRATION OF THE FEMUR DURING TOTAL HIP ARTHROPLASTY AND THE APPLICATION OF A DYNAMIC VIBRATION ABSORBER
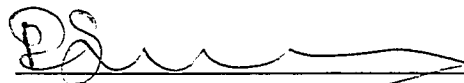
by

## Charles Ellis Ragan, IV

A THESIS SUBMITTED
IN PARTIAL FULFILLMENT OF THE
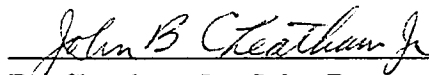REQUIREMENTS FOR THE DEGREE

## Master of Science

APPROVED, THESIS COMMITTEE:

Dr. Akin, John E., *Chairman*
Professor, Mechanical Engineering and
Materials Science

Dr. Spanos, Pol D.
Professor, Mechanical Engineering and
Materials Science

Dr. Cheatham Jr., John B.
Professor, Mechanical Engineering and
Materials Science

Dr. Harrigan, Timothy P.
Visiting Professor, Mechanical
Engineering and Materials Science

Houston, Texas

May, 1995

UMI Number: 1377048

# UMI

300 North Zeeb Road
Ann Arbor, MI 48103

# Abstract

# VIBRATION OF THE FEMUR DURING TOTAL HIP ARTHROPLASTY AND THE APPLICATION OF A DYNAMIC VIBRATION ABSORBER

by

**Charles Ellis Ragan, IV**

The problem of femoral vibration during the reaming process in total hip arthroplasty is examined. These vibrations are modeled as the transverse vibration of a free-simple Euler-Bernoulli beam using a transfer matrix method which allows the calculation of the frequency response of the beam. This method also allows for the calculation of the response when a dynamic vibration absorber is attached. Based on these calculations, a finite element model of the vibration absorber is developed and then an experimental prototype of a damper which could be used during the surgery is made. Tests are performed with real cadaveric femurs for cases with and without the vibration absorber. Then the frequency response is calculated from these experiments and compared with the calculated values. Based on these preliminary results, it appears that by properly selecting a vibration absorber, the magnitudes of the femoral vibrations can be significantly reduced.

# Acknowledgments

# Table of Contents

# List of Figures

vii

# Nomenclature

| Term | Explanation |
|------|-------------|
| A-P | anterior-posterior |
| CT | computed tomography |
| DOF | degree of freedom |
| DVA | dynamic vibration absorber |
| M-L | medial-lateral |
| THA | total hip arthroplasty |
| accelerance | output accelerance per unit force input, typically plotted against frequency |
| acetabulum | "the large cup shaped cavity ... in which the head of the femur articulates" |
| calcar | "the plate of strong tissue which strengthens the neck of the femur" |
| cancellous | "of a reticular, spongy, or lattice-like structure" |
| cortical bone | hard, dense bone comprising the outer layer of the femur |
| greater trochanter | "a broad flat process at the upper end of the lateral surface of the femur to which several muscles are attached" |
| intramedullary | "within the marrow cavity of a bone" |
| lateral | "denoting a position farther from the median plane or middle of the body or of a structure" |
| medial | "pertaining to the middle; closer th the median plane or the midline of a body or structure" |
| receptance | output displacement per unit force input, typically plotted against frequency |
| $c$ | damping , force/velocity |
| $E$ | Young's modulus (modulus of elasticity) |
| $F$ | shear force |

I              "area moment of inertia of beam cross section about beam's neutral axis" [2]

k              spring constant, force/length

m             mass

M             bending moment

Y, y          displacement

Z             state vector, where

$$\mathbf{Z_k^T} = \{ \mathbf{F_r} \quad \mathbf{M_r} \quad \phi_r \quad \mathbf{Y_r} \quad \mathbf{F_i} \quad \mathbf{M_i} \quad \phi_i \quad \mathbf{Y_i} \}_k$$

$\phi$             slope of beam

$\zeta$             percent critical damping, where $c_{cr} = 2\sqrt{mk}$

Note: the medical definitions are from [1]

# Chapter 1

# Introduction and Background

## 1.1  Brief History and Types of Hip Implants

Hip replacement surgery, or more accurately, total hip arthroplasty (THA), is the replacement of the femoral head and the acetabulum with artificial components, as indicated, in general, by the failure of the ball and socket joint due to bone deterioration or fracture. The replacement of the head of the femur with a prosthesis involves the removal of the femoral head and the insertion of a (generally) metal implant into the femoral canal. An artificial femoral ball is attached to the end of this implant, and this ball rotates in an artificial acetabular cup which is typically made of high-density polyethelene and mounted into the patient's acetabulum. The materials of which both of these components are made, and the method of their attachment to the existing bone, and the long term effects of these choices are the subjects of considerable study and debate.

Of particular interest here is the method of affixing the femoral component to the remaining bone, because deficiencies in all of the current methods are significant motivators for this study. There are basically three systems at this time: cemented, cementless, and custom. Clearly, the needs of each patient must be considered in determining which method will be used, and each system has its own strengths and weaknesses.

Cemented components were the first type used when Glück performed the first THA using ivory components in the 1890's. In 1960 Sir John Charnley made a huge

contribution to hip replacement surgery in when he began using methyl methacrylate cement – a self curing acrylic cement which markedly improved the fixation of the femoral component. Charnley began using this cement not merely as a glue, as others had done, but as a "grout," where it acted as the interface between the implant and the bone around the entire surface of the implant. This thicker coat of cement contributed to the higher success rate of his implants [3]. This technique is still in use and frequently produces very good results, especially in the initial period after implantation [4]. Some significant concerns do exist, however, such a the failure of the cement over time, which leads to revision surgery with a much lower success rate [5]; the potential systemic effects of acrylic bone cement [6] ; and the loss of bone due to stress shielding because of the way in which the implant is secured [4]. See Figure 1.1 [6] for one of Charnley's cemented implants.

Uncemented implants can be divided into two groups: press fit implants which depend on friction, and therefore extensive contact, between the implant and the bone, and bone-ingrowth implants which rely on the formation of new bone either into pores or around geometric features on the implant's surface. The drawback to uncemented implants is that despite their potential for better long-term results, given the elimination of the failure modes associated with the cement, their long-term success is not yet proven [7]. This is due to the extreme necessity for rigid initial fixation [8],[9]. Press fit implants depend on this mechanical rigidity from the time of their insertion onward, while bone-ingrowth prostheses rely on it until new bone is formed to further secure them in the femoral canal. It has been shown that the distance between the hip and the bone seems to impact both the amount and the speed of bone ingrowth into the prosthesis. Gaps over 2 mm appear to prevent

**Figure 1.1:** A Cemented Hip Implant

bone ingrowth, while gaps under 0.5 mm aid it noticeably [10]. Figure 1.2 shows an uncemented implant [8].

Custom prostheses are those developed uniquely for an individual patient, generally by using computed tomography (CT) scan data in combination with computer modeling software for the design and manufacture of the component [11]. The shape of the implant is generally designed to maximize the "fit," or agreement in shape between the prosthesis and the existing bone, and the "fill," or portion of the canal occupied by the implant [11],[12], although there is significant variance in the exact criteria used for the design [4]. The use of these custom components seems to be particularly indicated when available non-custom components do not match the patient's bone geometry sufficiently well [11]. The potential disadvantages of these

**Figure 1.2:** An Example of an Uncemented Femoral Implant

custom implants include concerns about the accuracy of the CT scans used to develop the implant, and the higher cost of the custom components. In addition, some undersizing of the implant may be unavoidable in order to make the implant insertable, thus defeating the original purpose [13]. In Figure 1.3 a custom implant is shown.

## 1.2 Uncemented Surgical Procedure

The surgical procedure for inserting an uncemented prosthesis should be considered in order to understand the mechanics and the implications of the methodology and changes which may be suggested by the study. The particular technique recommended by Engh and Bobyn is discussed here, although the general principles, particularly in regard to the reaming of the femoral canal, remain the same. First, the surgeon makes

**Figure 1.3:** An Example of a Custom Hip Implant by Wright Medical

an incision along the lateral side of the patient's buttock, and after detaching the appropriate muscles and ligaments, removes the ball of the femur from the hip socket. At this point, there is some variation in technique as to the order of the surgical procedure, but Engh recommends that before the preparation of the acetabular region, the pilot hole for the reamers which will eventually be used to size the femoral canal be drilled [8]. Generally, however, the femoral head is removed prior to reaming the canal, and this variation is an important point to consider for the purposes of this study. Once the pilot hole is made and a high speed burr has been used to remove some cortical bone from the greater trochanter, intramedullary reamers with successively greater diameters are used to widen the canal in preparation for the implant. The canal should be made exactly the same diameter as the cylindrical portion of the

femoral component. The goal of the reaming is to provide a tight fit for the distal portion of the prosthesis into the cortical bone of the femur, as essentially all of the distal cancellous bone is removed. The reamers are precisely sized to correspond to the proper implant and have a rounded end so that no inadvertent cutting of the cortical bone occurs and so that only the sides of the tool remove bone. Additionally, the cutting surfaces extend for the entire length of the reamer so that the hole is a constant diameter and to eliminate the potential for misalignment at the distal end of the reamer once the canal had been widened proximally. Figure 1.4 is an illustration of the proper reamers to use in contrast with one which will allow too much bone to be removed from the canal [8]. It is this portion of the surgery which is emphasized by this study.

After the femoral canal is prepared, appropriate measurements are made for the alignment of the implant, and the head of the femur is removed, if this has not been done already. Surgical chisels, burrs and rasps are used to remove bone in the proximal femur and the femoral neck for the insertion of the upper, triangular portion of the implant.

After a trial prosthesis, which is somewhat smaller than the actual one, is inserted to provide the surgeon with a check for proper preparation, the actual prosthesis is hammered into place. A tight fit is desired as has been discussed, but not so tight that the femur is fractured [8].

In addition to the femoral component, a cup, typically made of a polyethelene insert in a metal backing is inserted and firmly anchored into the patient's acetabulum, that is, the hip socket [8].

INTRAMEDULLARY
DRILLING

YES

NO
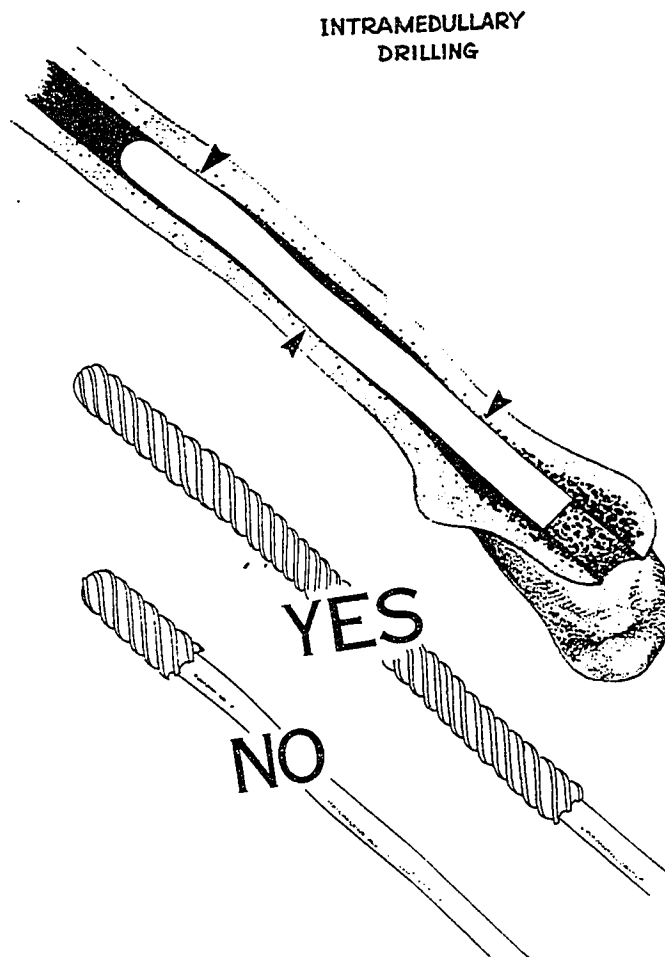
Figure 1.4: Proper and Improper Reamers

## 1.3 Significance of Precision

As has been discussed, the precision of the fit of the femoral component into the intramedullary canal is a critical factor in the successful outcome of the THA. Underreaming can result in the fracture of the femur when the prosthesis is impacted into its final position. Overreaming can lead to a number of negative consequences.

The gap between the bone and the implant can be too large to allow bony ingrowth. In addition, even very slight motion of the prosthesis in the canal, known as micromotion, can inhibit bony ingrowth in much the same fashion as motion at a fracture prevents its healing [8]. Furthermore, this motion can cause the deterioration of the implant itself [14], and this poses histological problems because of the potential health hazards related to free metallic ions from the alloys typically used in these implants, in addition to the more obvious mechanical problems. The presence of these metallic particles may lead to additional bone damage and resorption [15]. Micromotion has also been linked to thigh pain in implant recipients [16].

In addition, if too much cortical bone is removed, the femur can be weakened and this can also lead to fracture. These dangers obviously preclude both the oversizing and undersizing of the canal. The vibrations produced by the reamer introduce inaccuracies into the preparation of the canal, as seen in the next chapter, and it is these vibrations which are the focus of this study and which present serious problems for the THA patient.

# Chapter 2

# Previous and Related Work

This current work is the last in a three year study which has focused on the specific concern of the vibration of the femur during the reaming operation which is done to ready the femoral canal for the implant insertion. This study has also attempted to provide a more general understanding of the mechanics of the reaming process and the interaction between the cutting tool and the bone.

The results from the previous research which are of the most importance here are the response characteristics of the femur to the forced vibration and the corresponding dynamic model of the surgical process. Based on these measurements of natural frequencies and and their corresponding mode shapes, one can construct a preliminary mathematical simulation of these vibrations. As this model is tested and refined, the effects of a dynamic vibration absorber (DVA) can be considered.

The dynamic behavior of the femur, its bending in the anterior-posterior (A-P) and medial-lateral (M-L) directions and rotation about the proximal-distal axis, was previously studied (at Truman Medical Center, Kansas City, Missouri) through the measurement of accelerometer response to recorded impulses which correspond to low band frequency excitation with known characteristics, and through accelerometer data taken during simulated surgical reaming of the femoral canal. All of these experiments were performed on cadaveric human legs. In addition to examining accelerometer response and thus determining the transfer function and natural frequencies of the femur, the reamed femoral canal was examined to determine the accuracy of the

reaming and to better evaluate the bending of the femur when excited by the reamer [17].

Although it is difficult to characterize the behavior of the femur because of its irregular cross section, the complex boundary conditions in effect, the significant variation between individuals [18] and the non-linear material properties of bone, certain conclusions and generalizations can be made based on the experimental data. Impulse response testing showed that in the M-L direction the first natural frequency tends to occur between 50 and 100 Hz. In the A-P direction, the first natural frequency tends to occur between 100 and 300 Hz. Higher natural frequencies in the bending modes occur above 400 Hz, and torsional modes also become apparent between 400 and 1200 Hz. There is significant variation between femurs, but these general trends provide useful information [17]. Figure 2.1 is the transfer function from a femur studied in one of the earlier phases of this study. Reaming tests, in which an orthopedic surgery resident performed the femoral reaming in a fashion typical of the actual surgery, are also instructive in several ways. The first observation is that the use of the smaller reamers, i.e. those under 13 mm in diameter, produces significantly different effects than the use of larger reamers because they are removing the softer tissues and the cancellous bone, which is an open celled material composed of interconnecting spicules, rather than the harder, denser cortical bone which makes up the outer surface of the femur. The larger reamers begin removing cortical bone at an average diameter of 13 mm and transmit more energy to the bone, much of it into torsional modes, some into A-P modes, and relatively little into the M-L direction. Interestingly, when the shape of the machined canal is examined by performing C-T scans and by cutting the femur cross-sectionally, it is seen to be oval shaped with the larger diameter in the A-P direction [17]. This oval shape seems to indicate that the
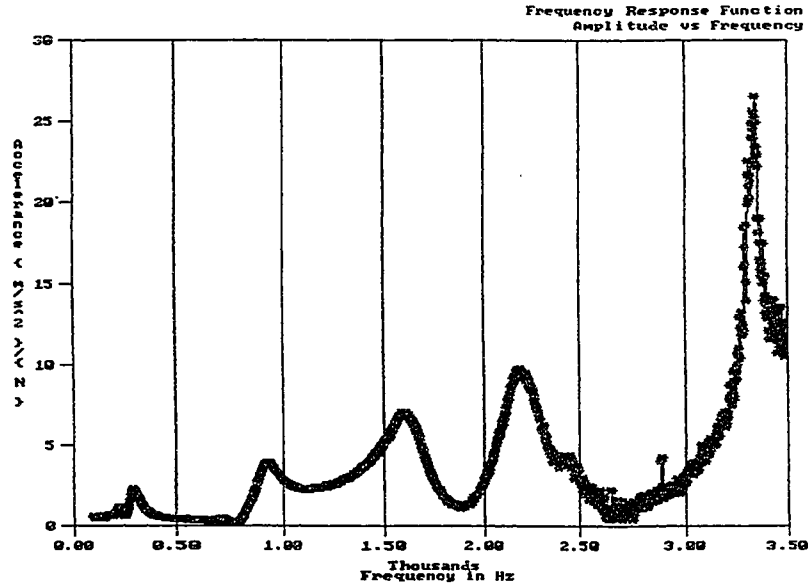
**Figure 2.1:** Accelerance vs Frequency for Femur, from Previous Portion
of Study

most important effect on the accuracy of the surgery is the A-P vibration of femur
as the reamer is cutting the cortical bone.

The magnitudes of these vibrations are the most pronounced at low frequencies,
as seen for a vibrating system described by

$$m\frac{d^2y(x,t)}{dx^2} + c\frac{dy(x,t)}{dt} + y(x,t) = f(t) \tag{2.1}$$

then

$$y = Y(x)e^{-i\omega t} \quad \text{and} \quad \frac{d^2y}{dt^2} = -\omega^2 y \quad \text{yielding} \quad y = -\frac{1}{\omega^2}\frac{d^2y}{dt^2} \tag{2.2}$$

so the magnitude of the displacement, $y$, is equal to the measured acceleration divided
by the square of the frequency. Because higher natural frequencies have increasingly
smaller effects on displacement, the first one or two natural frequencies of the femur

are of the most interest. Natural frequencies greater than 1KHz produce responses of less than 10 microns, and can be neglected here [19].

Based on these general trends, a representation of a "standard" femur can be developed in order to model its vibration characteristics and the effect of a damping device mathematically. For this case, the first two natural frequencies are taken as approximately 300 and 900 Hz. If the femur is considered to be a uniform Euler-Bernoulli beam vibrating laterally in the A-P direction, it can be seen that these natural frequencies correspond nicely to the theoretical ones, if realistic values for the mechanical properties and dimensions of the femur are chosen, and if reasonable assumptions about the boundary conditions are made. This analysis will be developed in detail in the following chapter.

It is appropriate to briefly note that some work by other researchers has been done in this area, although these results have been at times conflicting [20], and it is hoped that this study will provide a solid foundation on which further research may be built.

# Chapter 3

# Analytical Model and Design of Damper

## 3.1 Euler-Bernoulli Beam Model

For an Euler-Bernoulli beam vibrating laterally in bending, the governing equation is

$$\frac{\partial^2}{\partial x^2}\left[EI\frac{\partial^2 y}{\partial x^2}\right] = -m\frac{\partial^2 y}{\partial t^2} \tag{3.1}$$

where $I$, $E$, and $m$ can vary with $x$ and where $y$ is a function of both $x$ and $t$ [21]. Figure 3.1 shows the beam and its coordinate frame.

Assuming a separable solution $y(x,t) = Y(x)f(t)$ yields

$$\frac{d^2}{dx^2}\left[EI\frac{d^2 Y(x)}{dx^2}\right] - \omega^2 m Y(x) = 0 \tag{3.2}$$

$$\frac{d^2 f}{dt^2} + \omega^2 f(t) = 0 \tag{3.3}$$
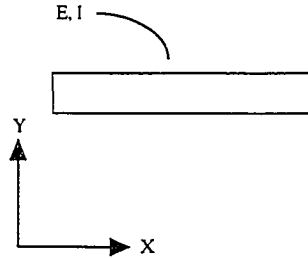
Figure 3.1: The Euler-Bernoulli Beam

Equation 3.2 has a solution of form

$$Y(x) = C_1 \sin \beta x + C_2 \cos \beta x + C_3 \sinh \beta x + C_4 \cosh \beta x \tag{3.4}$$

with

$$\beta^4 = \frac{\omega^2 m}{EI} \tag{3.5}$$

The squares of the natural frequencies are the eigenvalues of such a system, and for a given set of boundary conditions, the mode shapes, $Y(x)$, which are the eigenfunctions, can be evaluated by solving the simultaneous equations which depend on the results of standard beam theory. That is,

$$M = EI \frac{\partial^2 y}{\partial x^2} = EI \frac{d^2 Y(x)}{dx^2} f(t) \tag{3.6}$$

$$Q = -\frac{\partial M}{\partial x} = -\frac{\partial}{\partial x} \left[ EI \frac{\partial^2 y}{\partial x^2} \right] \tag{3.7}$$

If such a beam of length L is constrained against translation but not rotation at one end and unconstrained in any way at the other end, it will be called a "simple-free" beam. Based on the relations above, its natural frequencies can be derived by solving the following set of simultaneous equations.

$$Y(0) = 0 \tag{3.8}$$

$$M(0) = 0 \tag{3.9}$$

$$M(L) = 0 \tag{3.10}$$

$$Q(L) = 0 \tag{3.11}$$

Given Equations 3.4, 3.6, and 3.7, and assuming a constant cross section and uniform material properties these become

$$C_2 + C_4 = 0 \tag{3.12}$$

$$-C_2\beta^2 + C_4\beta^2 = 0 \qquad (3.13)$$

$$-C_1\beta^2 \sin\beta L - C_2\beta^2 \cos\beta L + C_3\beta^2 \sinh\beta L + C_4\beta^2 \cosh\beta L = 0 \qquad (3.14)$$

$$-C_1\beta^3 \cos\beta L + C_2\beta^3 \sin\beta L + C_3\beta^3 \cosh\beta L + C_4\beta^3 \sinh\beta L = 0 \qquad (3.15)$$

[21].

At this point it is convenient to either solve these equations via computer, or to reference the complete solution tables for this problem published by Young and Felgar [22] or condensed versions such as in [2]. These tables show that

$$\omega_n = \frac{X_n^2}{L^2}\sqrt{\frac{EI}{\rho S}} \qquad (3.16)$$

where $S$ is the cross sectional area of the beam and where $X_n^2 = 15.41, 49.96$ for a simple-free beam [2].

If $E = 20\text{x}10^9$ Pa, which is at the upper end of the range of what is considered to be the modulus of elasticity for bone [23] and $\rho = 2000$ kg/m$^3$, which is an adequate approximation of bone's density, then a hollow cylinder of length $L = 0.42$ m with constant cross-section and $d_i$=0.0214 m (27/32") and $d_o$=0.0254 (1") will yield natural frequencies of $\omega_1 = 279.7$ Hz and $\omega_2 = 906.7$ Hz. These frequencies are in approximate agreement with those of the "standard" femur from the previous chapter, based on these reasonable values for the physical parameters.

The assumption of simple-free boundary conditions is given some credibility by this result, but these conditions are also descriptive of the surgical scenario. The hip has been removed from the socket, and the head of the femur is unconstrained. The knee joint is a hinge allowing rotation in the A-P plane, and although a member of the surgical team attempts to keep the leg fixed by holding the knee during the reaming of the femoral canal, it is reasonable to believe that the translational rotation

will be more effectively constrained than rotation about the hinge joint. While this is not a rigorous justification, it does give some insight into what is occurring, and also provides a starting point from which to work.

Now that the problem has been simplified somewhat to the point that it can be modeled analytically, a more sophisticated technique can be used to examine the femur's response. In addition, the effects of attached masses and DVA's with spring, mass, and dashpot components can be calculated. This technique is known as the transfer matrix method, and it is an application of work first done by Holzer and Mykelstad and later expanded by Pestel and Leckie [26]. First, however, a brief summary of DVA theory is useful.

## 3.2    Summary of Dynamic Vibration Absorber Theory

The DVA is a secondary vibrating system which is attached to the primary system under consideration. Correctly tuning it by adjusting its effective parameters, m, k, and c, allows it to vibrate when the primary system is excited such that the motion of the primary system is reduced or eliminated. In an ideal single degree of freedom system when a vibration absorber is attached as in Figure 3.2, the equations become

$$m_1\ddot{x}_1 + (k_1 + k_2)x_1 - k_2x_2 = F_1 \sin\omega t \qquad (3.17)$$

$$m_2\ddot{x}_2 - k_2x_1 + k_2x_2 = 0 \qquad (3.18)$$

which has a solution of form

$$x_1(t) = X_1 \sin\omega t \quad\text{and}\quad x_2(t) = X_2 \sin\omega t \qquad (3.19)$$

which gives

$$\begin{bmatrix} k_1 + k_2 - \omega^2 m_1 & -k_2 \\ -k_2 & k_2 - \omega^2 m_2 \end{bmatrix} \begin{bmatrix} X_1 \\ X_2 \end{bmatrix} = \begin{bmatrix} F_1 \\ 0 \end{bmatrix}$$

and yields

$$X_1 = \frac{(k_2 - \omega^2 m_2)F_1}{(k_1 + k_2 - \omega^2 m_1)(k_2 - \omega^2 m_2) - k_2^2} \qquad (3.20)$$

$$X_2 = \frac{(k_2 F_1)}{(k_1 + k_2 - \omega^2 m_1)(k_2 - \omega^2 m_2) - k_2^2}. \qquad (3.21)$$

It can be seen from the numerator, that if $k_2$ and $m_2$ are chosen such that $\sqrt{\frac{k_2}{m_2}} = \omega$ then $X_1 = 0$ [24].

When dashpots are included, the analysis becomes more complicated, and the amplitude of the primary mass cannot be reduced to zero, but appropriate tuning can considerably reduce the vibration of the primary mass at the forcing frequency, although the peak at $\omega$ will be shifted into two peaks at $\omega_1$ and $\omega_2$, the exact shapes of which are determined by the damping. Figure 3.3 shows how the peaks are shifted by the absorber and the effect of damping [25].
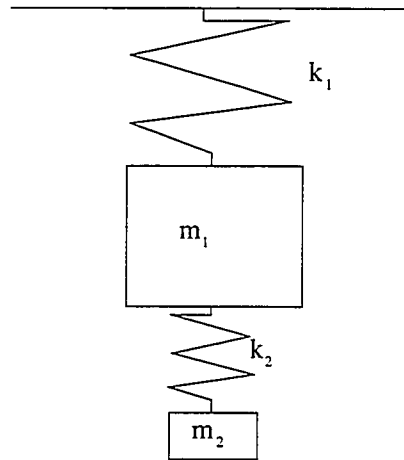


**Figure 3.2:** A Single Degree of Freedom System with Vibration Absorber
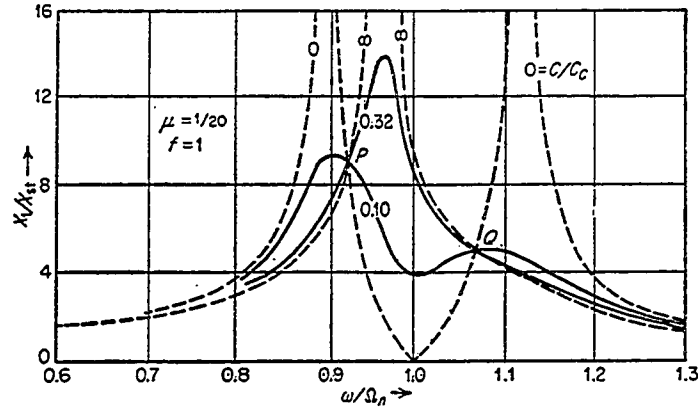
**Figure 3.3:** Frequency Response of 1 DOF system with DVA and Various Damping Values

## 3.3 Transfer Matrix Method: Theory

For a vibrating system with a given state vector $\mathbf{Z}$ describing its condition at a point, namely its displacement, angular rotation, bending moment, and shear force, the state vector at another point in the system can be determined through the relationship,

$$\mathbf{Z}_{k+1} = \mathbf{T}_k \mathbf{Z}_k \quad \text{where} \quad \mathbf{Z}_k^{\mathbf{T}} = \{\mathbf{F} \quad \mathbf{M} \quad \phi \quad \mathbf{Y}\}_k \qquad (3.22)$$

provided that the transfer matrix $\mathbf{T}$ is known between points $k$ and $k+1$. For a system made up multiple elements, then [27]

$$\mathbf{Z}_{\mathbf{N}} = \mathbf{T}_{\mathbf{N}-1} \cdots \mathbf{T}_2 \mathbf{T}_1 \mathbf{Z}_1 \quad \text{where} \quad \mathbf{Z}_i^{\mathbf{T}} = \{\mathbf{F} \quad \mathbf{M} \quad \phi \quad \mathbf{Y}\}_i \qquad (3.23)$$

Pestel and Leckie [26] have computed transfer matrices for a number of different mechanical elements, including beams, attached masses, and attached DVA's, and Seto [27] has used these matrices in the solution of a dynamic vibration absorber
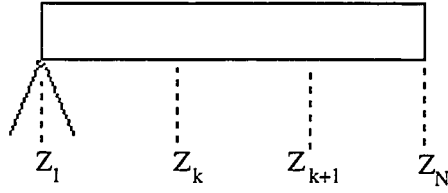
**Figure 3.4:** Simple-Free Beam with State Vector **Z**

problem. These transfer matrices provide an exact analytical solution to the problem, rather than the approximate solution which would be reached through the use of finite elements or another approximate computational method.

For details of their derivation see [26]. The following are the transfer matrices used, in a somewhat different form than given in [27]. They are given in a form with the first four rows corresponding to the real components of the state vector, and the second four rows corresponding to the imaginary components. This would be unnecessary were it not for the dashpot in the DVA which introduces imaginary terms into the transfer matrices. It is more efficient computationally to then create an 8x1 state vector with real and imaginary components, and to modify the transfer

matrix accordingly. The state vector $Z$ is such that

$$\mathbf{Z_k^T} = \{\mathbf{F_r} \quad \mathbf{M_r} \quad \phi_{\mathbf{r}} \quad \mathbf{Y_r} \quad \mathbf{F_i} \quad \mathbf{M_i} \quad \phi_{\mathbf{i}} \quad \mathbf{Y_i}\}_k \tag{3.24}$$

Each transfer matrix is a function of both the physical properties of the system and the frequency at which it is excited.

Beam segment of mass $m_b$ and length $l$: where

$$S = (\cosh \lambda l + \cos \lambda l)/2 \tag{3.25}$$

$$T = (\sinh \lambda l + \sin \lambda l)/2 \tag{3.26}$$

$$U = (\cosh \lambda l - \cos \lambda l)/2 \tag{3.27}$$

$$V = (\sinh \lambda l - \sin \lambda l)/2 \tag{3.28}$$

$$\lambda = \frac{m_b \omega^2}{EIl} \tag{3.29}$$

$$T_b = \begin{bmatrix} S & -\lambda V & EI\lambda^2 U & -EI\lambda^3 T & 0 & 0 \\ -T/\lambda & S & -EI\lambda V & EI\lambda^2 U & 0 & 0 \\ U/EI\lambda^2 & -T/EI\lambda & S & -\lambda V & 0 & 0 \\ -V/EI\lambda^3 & U/EI\lambda^2 & -T/\lambda & S & 0 & 0 \\ 0 & 0 & 0 & 0 & S & -\lambda V \\ 0 & 0 & 0 & 0 & -T/\lambda & S \\ 0 & 0 & 0 & 0 & U/EI\lambda^2 & -T/EI\lambda \\ 0 & 0 & 0 & 0 & -V/EI\lambda^3 & U/EI\lambda^2 \end{bmatrix}$$

$$\left. \begin{array}{cc} 0 & 0 \\ 0 & 0 \\ 0 & 0 \\ 0 & 0 \\ EI\lambda^2 U & -EI\lambda^3 T \\ -EI\lambda V & EI\lambda^2 U \\ S & -\lambda V \\ -T/\lambda & S \end{array} \right] \tag{3.30}$$

Attached DVA composed of spring-mass-damper combination with

mass $m_d$, spring $k_d$, and damper $c_d$:

$$T_{DVA} = \begin{bmatrix} 1 & 0 & 0 & N_R/D & 0 & 0 & 0 & -N_I/D \\ 0 & 1 & 0 & 0 & 0 & 0 & 0 & 0 \\ 0 & 0 & 1 & 0 & 0 & 0 & 0 & 0 \\ 0 & 0 & 0 & 1 & 0 & 0 & 0 & 0 \\ 0 & 0 & 0 & N_I/D & 1 & 0 & 0 & N_R/D \\ 0 & 0 & 0 & 0 & 0 & 1 & 0 & 0 \\ 0 & 0 & 0 & 0 & 0 & 0 & 1 & 0 \\ 0 & 0 & 0 & 0 & 0 & 0 & 0 & 1 \end{bmatrix} \tag{3.31}$$

with the defining relationships

$$\omega_d = \sqrt{k_d/m_d} \tag{3.32}$$

$$\zeta = c_d/2\sqrt{m_d k_d} \tag{3.33}$$

$$N_R = \omega_d^2 \left( \omega_d^2 - \omega^2 \right) + (2\zeta\omega_d\omega)^2 \tag{3.34}$$

$$N_I = 2\zeta\omega_d\omega^3 \tag{3.35}$$

$$D = -\left[\left(\omega_d^2 - \omega^2\right)^2 + (2\zeta\omega_d\omega)^2\right]/m_d\omega^2 \qquad (3.36)$$

Attached mass of mass $m_a$:

$$T_a = \begin{bmatrix} 1 & 0 & 0 & -m_a\omega^2 & 0 & 0 & 0 & 0 \\ 0 & 1 & 0 & 0 & 0 & 0 & 0 & 0 \\ 0 & 0 & 1 & 0 & 0 & 0 & 0 & 0 \\ 0 & 0 & 0 & 1 & 0 & 0 & 0 & 0 \\ 0 & 0 & 0 & 0 & 1 & 0 & 0 & -m_a\omega^2 \\ 0 & 0 & 0 & 0 & 0 & 1 & 0 & 0 \\ 0 & 0 & 0 & 0 & 0 & 0 & 1 & 0 \\ 0 & 0 & 0 & 0 & 0 & 0 & 0 & 1 \end{bmatrix} \qquad (3.37)$$

## 3.4 Transfer Matrix Method: Implementation

By applying these principles a FORTRAN computer program was developed which reads in user defined attributes of a system composed of the three above element types. The program calculates the element and the system transfer matrix for each frequency in a range defined by the user. Given the system transfer matrix and the simple-free boundary conditions, a sinusoidal excitation of magnitude 1 is applied at the free end to simulate the vibrations induced by the reamer. Four of the resulting equations are solved simultaneously for the real and imaginary components of the the force and the slope at the simple support of the beam. These values are then inserted back into the main equation to solve for displacement at the free end. This is done for every frequency in the range, and because the exciting force is unity, the values for displacement are also the values for receptance in m/N.

Mathematically speaking,

$$
\begin{bmatrix} 1 \\ 0 \\ \phi_r \\ y_r \\ 0 \\ 0 \\ \phi_i \\ y_i \end{bmatrix}_N =
\begin{bmatrix}
T_{11} & T_{12} & T_{13} & T_{14} & T_{15} & T_{16} & T_{17} & T_{18} \\
T_{21} & T_{22} & T_{23} & T_{24} & T_{25} & T_{26} & T_{27} & T_{28} \\
T_{31} & T_{32} & T_{33} & T_{34} & T_{35} & T_{36} & T_{37} & T_{38} \\
T_{41} & T_{42} & T_{43} & T_{44} & T_{45} & T_{46} & T_{47} & T_{48} \\
T_{51} & T_{52} & T_{53} & T_{54} & T_{55} & T_{56} & T_{57} & T_{58} \\
T_{61} & T_{62} & T_{63} & T_{64} & T_{65} & T_{66} & T_{67} & T_{68} \\
T_{71} & T_{72} & T_{73} & T_{74} & T_{75} & T_{76} & T_{77} & T_{78} \\
T_{81} & T_{82} & T_{83} & T_{84} & T_{85} & T_{86} & T_{87} & T_{88}
\end{bmatrix}
\begin{bmatrix} F_r \\ 0 \\ \phi_r \\ 0 \\ F_i \\ 0 \\ \phi_i \\ 0 \end{bmatrix}_1
\tag{3.38}
$$

Solving for the unknowns at the support,

$$
\begin{bmatrix} F_r \\ \phi_r \\ F_i \\ \phi_i \end{bmatrix}_1 =
\begin{bmatrix}
T_{11} & T_{13} & T_{15} & T_{17} \\
T_{21} & T_{23} & T_{25} & T_{27} \\
T_{51} & T_{53} & T_{55} & T_{57} \\
T_{61} & T_{63} & T_{65} & T_{67}
\end{bmatrix}^{-1}
\begin{bmatrix} 1 \\ 0 \\ 0 \\ 0 \end{bmatrix}_N
\tag{3.39}
$$

And then substituting the now known values of $F$ and $\phi$,

$$
\begin{bmatrix} \phi_r \\ y_r \\ \phi_i \\ y_i \end{bmatrix}_N =
\begin{bmatrix}
T_{31} & T_{33} & T_{35} & T_{37} \\
T_{41} & T_{43} & T_{45} & T_{47} \\
T_{71} & T_{73} & T_{75} & T_{77} \\
T_{81} & T_{83} & T_{85} & T_{87}
\end{bmatrix}
\begin{bmatrix} F_r \\ \phi_r \\ F_i \\ \phi_i \end{bmatrix}_1
\tag{3.40}
$$

The code was initially based on a program given in [2] and then modified based on [27]. The full source code and input files are in Appendix A. For the "standard" femur discussed earlier it produced the receptance plot for the free end of the beam which is in Figure 3.5. Note the peaks at roughly 300 and 900 Hz. Because this is an
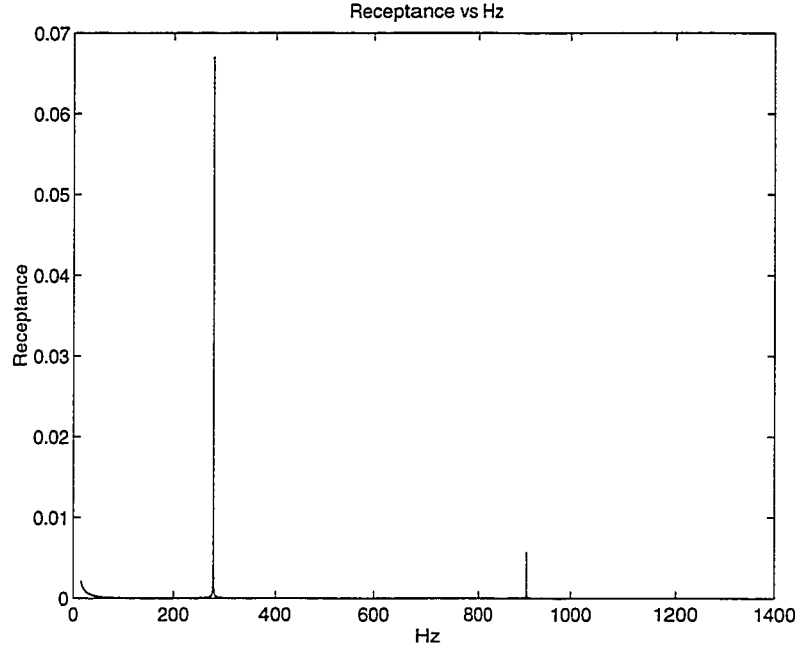
**Figure 3.5:** Plot of Receptance vs Frequency for End of Beam, Without DVA

analytical solution it agrees exactly with the the earlier calculated values and only requires a single beam "element."

Based on these predictions, multiple models of the same basic femur with varying attached masses and DVA's were run to get a good idea of how the beam's response would be effected. For example, the same femur with an attached mass of $m_a = 0.0171$ kg attached at the free end along with a DVA with $m = 0.0036$ kg, $k = 1.1734x10^4$ N/m, and $c = 0$,then the following response is obtained in Fig 3.6. Similarly, if the DVA is changed such that $\zeta = .02$, but all other properties remain the same, then the response is in Figure 3.7 .

Utilizing these tests, the general properties of the necessary DVA can begin to be formulated. An absorber with even a small amount of damping and a natural
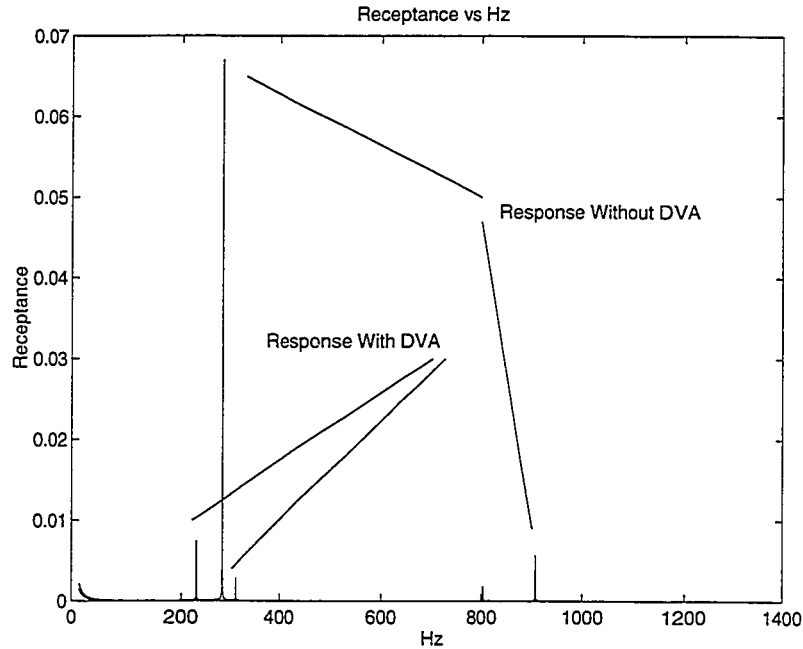
**Figure 3.6:** Plot of Receptance vs Frequency for End of Beam, With Attached Mass and DVA

frequency approximately equal to the natural frequency which is desired to be eliminated should successfully eliminate almost all of the response at the first natural frequency. It will also significantly reduce the response at the second natural frequency. It is important to see that this occurs without introducing any new peaks which, if created, would defeat the purpose of the absorber.

## 3.5 Development of Dynamic Vibration Absorber

Given that a DVA needs to meet the above criteria and also must be capable of being mounted to the bone, several different factors must be considered. First, it must have the correct mass and stiffness properties. Second, it should have a reasonably large $\zeta$.
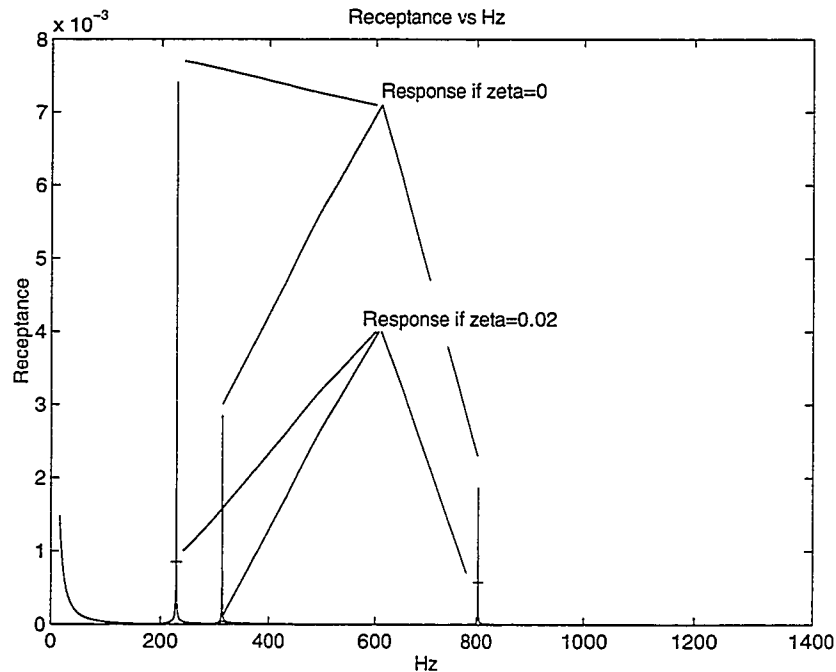
**Figure 3.7:** Plot of Receptance vs Frequency for End of Beam, With Attached Mass and Two Different DVA's

Finally, it should be usable in a surgical environment without introducing too many changes to the existing technique.

One of the first possibilities considered for the DVA was a cantilever beam which could be adjusted to account for variations between different person's femurs by adding weights to the end of the beam. The properties of such a clamped-free cantilever can be calculated by using a program similar to the one used for the femur itself. One problem with this design was a difficulty in securely affixing it to the bone and making certain that no stiffness was lost at the interface between the beam and the bone or in the intervening bracket which would be used to attach such a cantilever. It is also difficult to control the amount of damping in a DVA like this,

and only a limited amount will occur due to losses at interfaces and small material nonlinearities. In addition, a beam hanging off to one side like this may introduce additional rotational moments about the bone's axis, and produce other undesirable motions. A DVA like this could also be difficult to use in a surgical setting, making its ultimate use merely theoretical.

The second design was significantly better in several ways. This design uses a rubber ring which fits around the bone as the equivalent spring, and a metal exterior ring as the equivalent mass. The high damping value of rubber is a significant benefit, and although exact specifications for many types of rubber are difficult to obtain due to the wide variety of custom rubber compounds, reasonably approximate values can be readily obtained. Finite element models of various potential designs of this type were made with Patran, and ABAQUS was used to calculate the natural frequencies and modes. This process was repeated until a design was found which had a natural frequency of approximately 300 Hz. In this design the inner rubber piece has an inner diameter of 1.0 inch and an outer diameter of 2.0 inches, and the outer aluminum part has an outer diameter of 2.25 inches. Both are 1 inch wide. See Figures 3.8 and 3.9 for illustrations of the damper and the output of the displacements calculated by ABAQUS. Note that it is because master degrees of freedom were not defined that the analysis does not show motion along only one axis. This is not important considering the cylindrical symmetry of the damper.

If a DVA having these properties is mounted to the ideal simple-free beam considered earlier, it has a similar response. The receptance plot can be seen in Figure 3.10.

Based on this analysis a damper was then fabricated using a custom rubber by Applied Rubber Technology. This actual damper varied somewhat with respect to
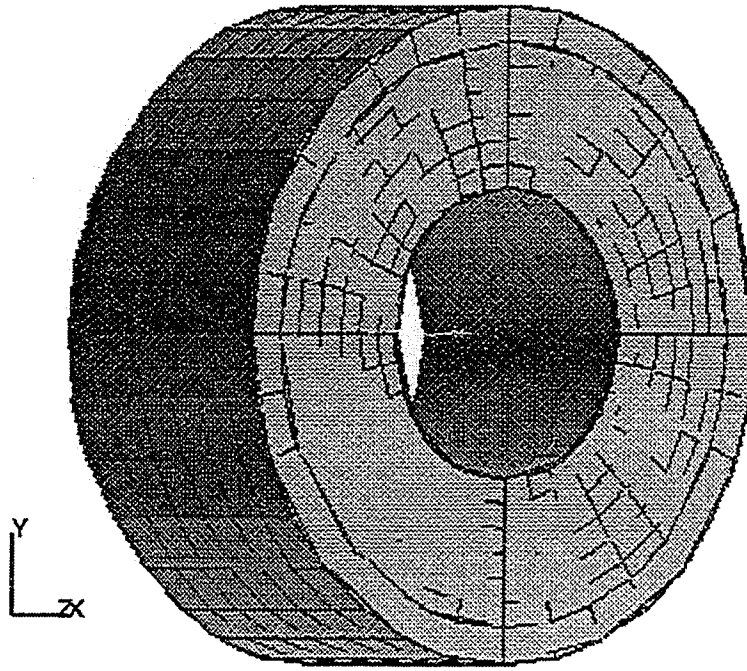
Figure 3.8: Patran model of DVA

the material properties of the rubber due to difficulty in matching the desired density

and modulus of elasticity exactly. In the analysis, the rubber was assumed to have

a density of 1196 kg/m³ and a Young's modulus of 1500 psi. The material specifica-

tion sheets available from the supplier did not specify the density, which is probably

close to the assumed value, and the elastic modulus is given as 1958 psi. Aluminum

sleeves were fabricated according to the design specified in the analysis. The actual

application of the DVA required additional modifications which are discussed in the

next chapter.
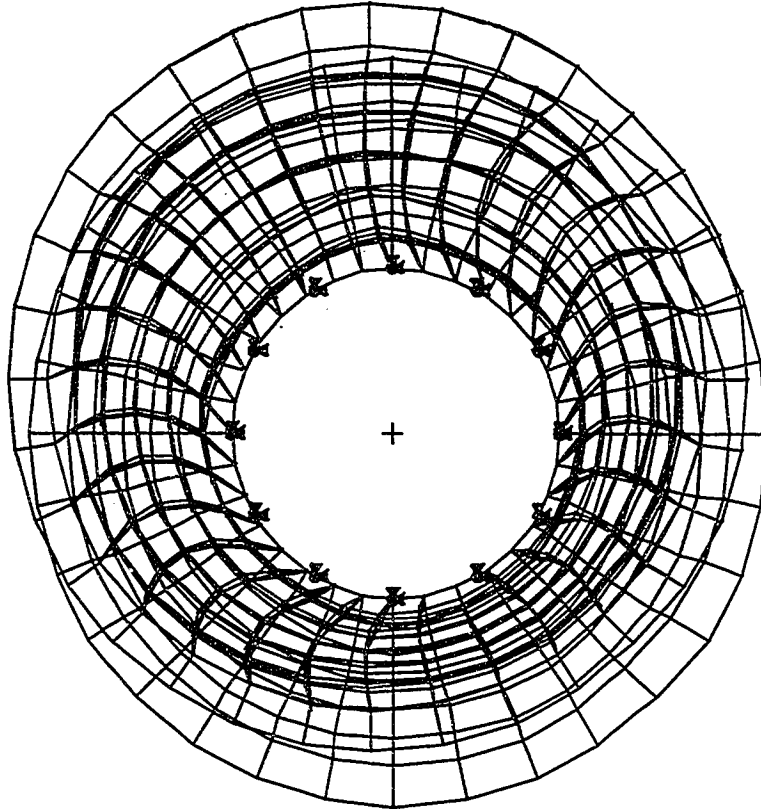
**Figure 3.9:** Displacements of DVA as calculated by ABAQUS

## 3.6    Possible Modifications to the Beam Model

It is worthwhile to note that a simple-free beam will respond to a constant force at any point along its length by rotating as a free body about its simply-supported end. However, an oscillating force acting at a point is not going to produce such free-body motion. Perhaps, though, given that it is desirable to completely exclude free body motion from the model, as this is not what occurs during surgery, and also given that the flesh surrounding the bone does act as some sort of spring support, it would be
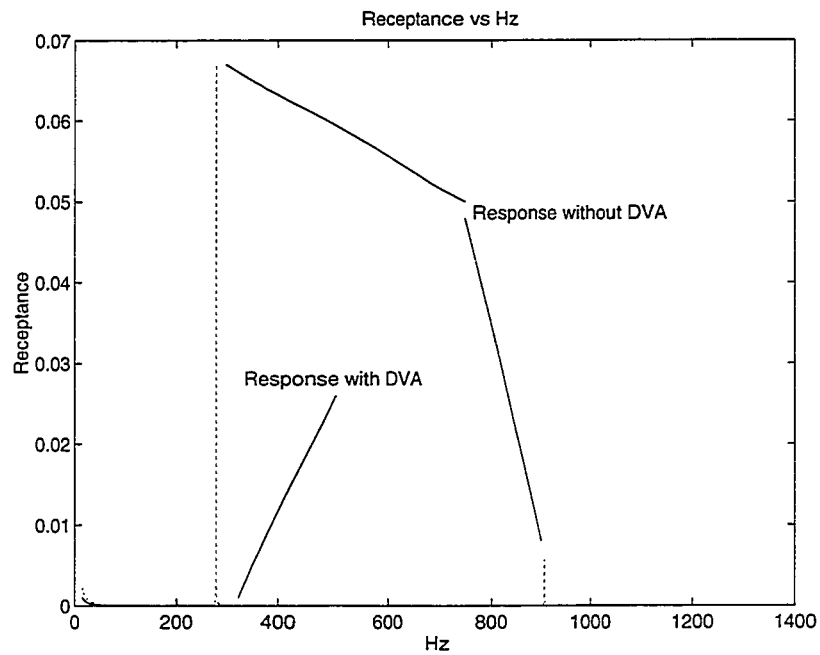
**Figure 3.10:** Receptance at End of Simple-Free Beam, Comparison With and Without Absorber Developed in Patran

good to consider the system as a simple-free beam supported on an elastic foundation with a stiffness per unit length of $\Gamma$.

This can be analyzed through the use of transfer matrices as above, where

$$
T = \begin{bmatrix}
c_0 & \beta^4\frac{c_3}{l} & \beta^4\frac{c_2}{a} & \beta^4\frac{c_1}{al} & 0 & 0 & 0 & 0 \\
lc_1 & c_0 & \beta^4 l\frac{c_3}{a} & \beta^4\frac{c_2}{al} & 0 & 0 & 0 & 0 \\
ac_2 & \frac{ac_1}{l} & c_0 & \beta^4\frac{c_3}{l} & 0 & 0 & 0 & 0 \\
alc_3 & ac_2 & lc_1 & c_0 & 0 & 0 & 0 & 0 \\
0 & 0 & 0 & 0 & c_0 & \beta^4\frac{c_3}{l} & \beta^4\frac{c_2}{a} & \beta^4\frac{c_1}{al} \\
0 & 0 & 0 & 0 & lc_1 & c_0 & \beta^4 l\frac{c_3}{a} & \beta^4\frac{c_2}{al} \\
0 & 0 & 0 & 0 & ac_2 & \frac{ac_1}{l} & c_0 & \beta^4\frac{c_3}{l} \\
0 & 0 & 0 & 0 & alc_3 & ac_2 & lc_1 & c_0
\end{bmatrix}
\tag{3.41}
$$

with

$$
\beta^4 = \frac{\rho S \omega^2 - \Gamma}{EI} l^4
\tag{3.42}
$$

$$
a = \frac{l^2}{EI}
\tag{3.43}
$$

$$
c_0 = \frac{1}{2}(\cosh\beta + \cos\beta)
\tag{3.44}
$$

$$
c_1 = \frac{1}{2\beta}(\sinh\beta + \sin\beta)
\tag{3.45}
$$

$$
c_2 = \frac{1}{2\beta^2}(\cosh\beta - \cos\beta)
\tag{3.46}
$$

$$
c_3 = \frac{1}{2\beta^3}(\sinh\beta - \sin\beta)
\tag{3.47}
$$

Interestingly, when this model is considered, the natural frequency peaks are not shifted visibly, and their magnitudes are only changed slightly. (See Figure 3.11) Therefore, it seems that the simple-free beam assumption has some merit, and the effect of the elastic foundation (the surrounding flesh) is to prevent free-body rotation from occurring.
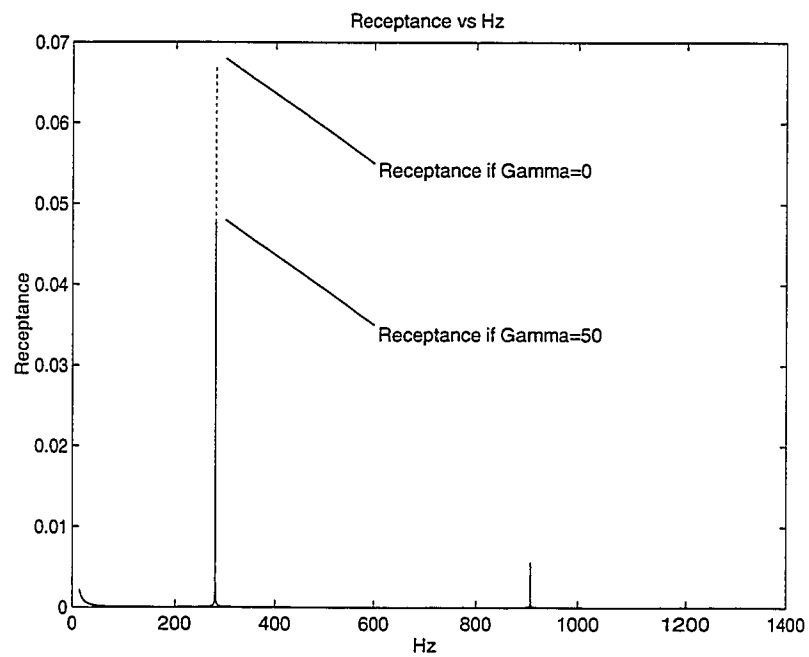
**Figure 3.11:** Receptance at End of Beam, With and Without Elastic Foundation

# Chapter 4

# Experimental and Data Processing Methods

Two types of experiments were performed. The first testing was done on whole cadaveric legs with the soft tissues largely intact such that the specimen closely resembled a patient in real surgery, and the surgical conditions were simulated as well as possible. In the second type of test the soft tissues were completely removed and the femur alone was studied while subjected to more reproducible boundary conditions. In all tests the material was unembalmed as an additional measure to achieve material characteristics as close as possible to those of living tissue.

## 4.1 Equipment

The primary equipment used to perform the testing consisted of Wilcoxon triaxial accelerometers, a PCB instrumented hammer, an Analogic data acquisition board mounted in an 80486 PC running Labtech Notebook data acquisition software. In addition, signals from the accelerometers were passed through a set of active filters with a cut off frequency of 10 Khz. To avoid aliasing, samples were taken at a rate of 20 Khz.

## 4.2 In Situ Testing

Impact tests were performed on two cadaveric legs. Prior to the attachment of the accelerometer the femoral head was removed in order to reproduce surgical conditions. This is because the presence of the femoral head would clearly affect the vibrational

characteristics of the bone. The accelerometer was attached to the femur by exposing the bone and drilling and tapping a small hole into a firm part of the bone approximately 6 cm below the calcar. This is the first suitable spot for the anchoring of an accelerometer, due to the brittleness of the bone and the irregularities of its surface proximal to this position. The instrumented hammer was used to excite the femur by striking it in the A-P direction at five marked intervals, 6 cm apart, along the length of the femur. The excitation values of the accelerations measured by the accelerometer in the hammer and the response measured by the accelerometer on the femur were stored on the PC after passing through the anti-aliasing filters and data acquisition card. Multiple tests at each point were performed to be certain that the data was captured properly. Due to equipment limitations, each run could only last 0.4 seconds at the 20 Khz sampling rate. This required that for each test the femur be struck repeatedly at a frequency in the neighborhood of 4 Hz to guarantee the successful capture of an input and response.

The second of the femurs used for impact testing was also tested with a DVA attached. Unfortunately, in order to attach the absorber additional thigh flesh was required to be cut away from the bone, making the situation somewhat less like the real surgical procedure, although it is not believed that this is a major contributor to the vibratory characteristics of the femur, based on the tentative results seen in Section 3.6 which seem to indicate that the stiffness of the elastic foundation does not appreciably affect the response. The absorber was attached just below the accelerometer, approximately 9 cm below the calcar cut, which was the first spot where it would fit, due to the non-circular and irregular shape of the femur above this point.

The actual DVA used was not ideal and only approximately matched the specifications of the Patran model. Specifically, both the inner and outer rings were cut across the diameter so that they could be attached around the bone. The irregularities of the most proximal portion of the femur prevent sliding the rings along the axis of the femur. Consequently, a hose clamp was used to secure these pieces to the femur. Finally, the rubber ring was not manufactured to fit the femur precisely, but was modified to do so in the lab with a scalpel. These irregularities obviously affect the exact characteristics of the DVA, but these tests are still useful for determining if the vibration of the femur can be significantly reduced with the use of a vibration absorber.

Reaming testing was done on only one femur because of difficulty in controlling the boundary conditions. The reaming tests done were on the second femur and actual surgical reamers were used in increasing sizes to ream the intramedullary canal. Equipment availability limited the use of the reamers, and an electric drill, rather than an air powered driver was used to power the reamers.

## 4.3  Testing of the Excised Femur

In order to compare the results of tests made under in-situ, and approximately surgical, conditions with results which would have greater reproducibility and less variation due to changes in technique between surgeons and between researchers, tests were also made on an excised femur as follows. The contralateral femur to that subjected to impact and reaming tests was excised and cleaned so that tests under more reproducible boundary conditions could be made. Tests were then performed subject to free-free and simple-free boundary conditions. As in the previous impact tests, an

accelerometer was mounted 6 cm below the calcar and the instrumented hammer was used to strike the femur at six intervals along its length.

In the free-free tests a string was used to suspend the femur vertically so that free-free conditions could be achieved. The string was tied to the femur such that a small amount of rotational stiffness was provided to prevent the impacts from creating too much swinging motion of the femur. Six locations along the length of the femur were used as impact points, starting at the accelerometer (6 cm below the calcar cut) and at five succeeding points, each 6 cm apart. The final impact point was 36 cm distal to the calcar, and was an additional point not used in the in situ tests.

For the simple-free tests, a jig composed of a rotating shaft supported by bearings mounted in a simple wooden frame was clamped to a lab table. The shaft was passed through a hole drilled in the tibial condyles in order to simulate the hinge joint at the knee. The other end of the femur was allowed to hang freely. Impact data was taken at the same six points as for the free-free test.

## 4.4   Data Processing

After the accelerometer time histories were stored by the PC, they were transferred to a UNIX workstation for analysis in MATLAB. The signals were normalized to remove small voltage offsets produced by the data acquisition board. Fast Fourier Transforms were then taken of each signal and the transfer function computed according to

$$X(\omega) = \frac{FFT(O)}{FFT(I)} \tag{4.1}$$

where $O$ is the time history of the accelerometer mounted on the femur, and $I$ is that of the instrumented hammer. $X(\omega)$ is the transfer function relating acceleration response to a given acceleration input. Acceleration input, however, is equal to

force input divided by a mass constant associated with the instrumented hammer. Therefore, $X(\omega)$ is seen to be equal to a constant times the accelerance. From the accelerance, the magnitude of the receptance can be calculated simply by dividing by $\omega^2$, as in Equation 2.2.

Finally, it is useful to compare the response at different points for a given exciting force, although the data is actually the response at one point for a variety of different exciting forces. The principle of reciprocity states that the response at a point A produced by an exciting force at point B is equivalent to the response at B due to an excitation at A. This principle allows the interpretation of data from a fixed accelerometer with different excitation points to be interpreted as the more useful response at multiple locations for a fixed exciting force. In the future discussion, this is how the data is interpreted.

# Chapter 5

# Experimental Results

## 5.1   In Situ Impact Test Results

### 5.1.1   Without DVA

For each data acquisition run, the time histories of the response of the hammer, which acts as the input function, and the response of all three axes of the accelerometer which is mounted on the femur, each of which are an output function, are recorded. Figure 5.1 shows one data set after the significant samples have been isolated. The large peak is the impulse produced by the instrumented hammer, and the second largest peaks are those from the A-P axis of the accelerometer. The remaining two channels are the response in the M-L and axial directions.

A number of tests were performed at each point, and these results are generally consistent for a given femur. Figures 5.2 and 5.3 demonstrate this. The differences in the high frequencies are due to limitations in the applicable range of the accelerometer's frequency response.

The transfer function for each channel is calculated as in Section 4.4. Because previous work has shown that the most significant vibrations occur in the A-P direction, the response along this axis was the main focus of the analysis. Plots of the transfer function for this axis at each point along the femur show a number of notable items about the dynamic response of each bone. The following figures show the transfer function of the second femur for the low frequency range of 0 to 1500 Hz at each of the "response" points along the length of the femur.
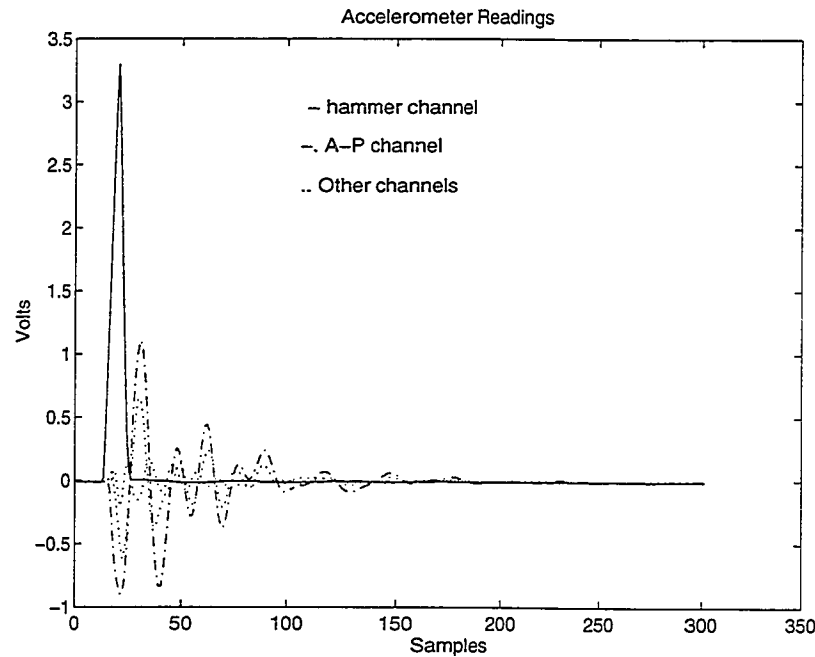
**Figure 5.1:** Sample Data from Accelerometers

First, a significant peak occurs in the range between 250 and 300 Hz. This peak is not visible at every measured point along the femur, but varies with location, as would be expected for a bending mode. It is difficult to say with certainty that this is the first bending mode of a simple-free beam, but it does share some characteristics with such a mode. The second major peak which occurs between 650 and 800 Hz also varies with location, but in a way different from the 300 Hz peak, giving further credibility to the proposition that these are bending modes. The lack of response near the middle of the femur seems to resemble a node like one which would be expected for the second mode of a simple-free beam.
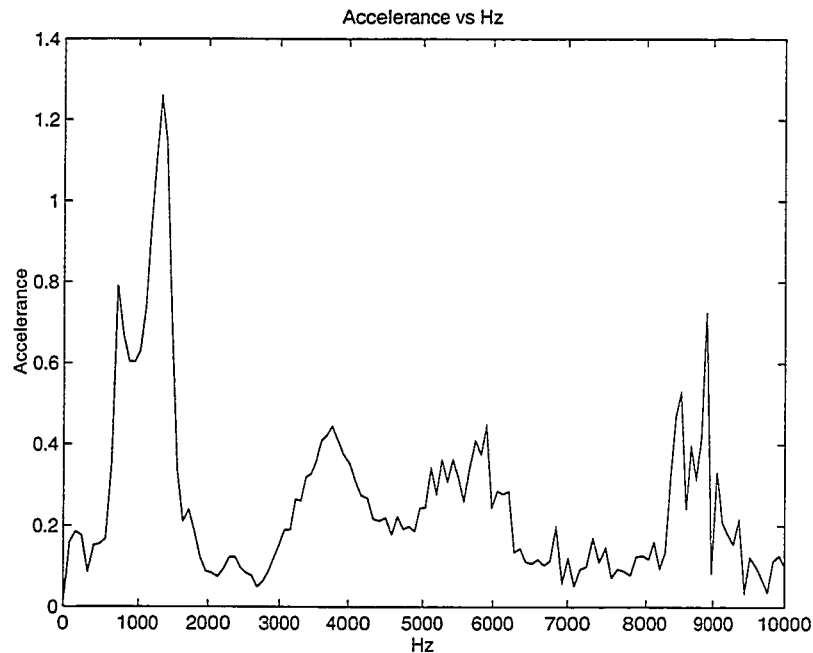
**Figure 5.2:** Accelerance vs Frequency for Femur #1 at 15 cm Below Calcar, Test #2

## 5.1.2  With DVA

When the DVA was placed approximately 9 cm below the calcar cut and the response of the femur was measured, a noticeable reduction in response was observed. This is particularly true at the 250 Hz peak, but is also quite evident at the 12 cm response point for the 667 Hz peak. At higher frequencies, the response is greater with the damper, but it is important to remember that this is only for accelerance, and that the displacement is negligible for these higher frequencies, as can be seen in Figure 5.7.
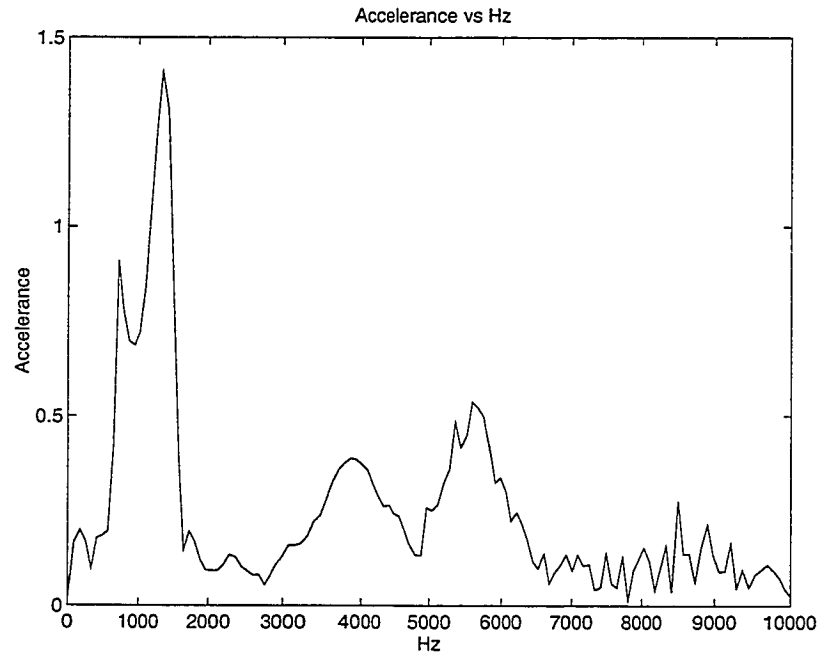
**Figure 5.3:** Accelerance vs Frequency for Femur #1 at 15 cm Below Calcar, Test #3

## 5.2  Reaming Test Results

The reaming tests results are primarily useful for demonstrating that a wide range of frequencies are excited in the bone. The primary limitation to these tests is the lack of certainty about the boundary conditions which are in effect and how these compare to those in actual surgery. It can be seen in the following plots that most of the energy is in the lower frequency range. In Figure 5.8, there is a medium sized peak in the Fourier amplitude of the acclerometer reading in the 300 Hz region, and a significant dip at 500 Hz which are both worth noting. The largest peak in this plot occurs around 1100 Hz, but this peak begins to grow in the 600 to 700 Hz range. It is apparent that significant energy exists in the region below 1500 Hz to excite
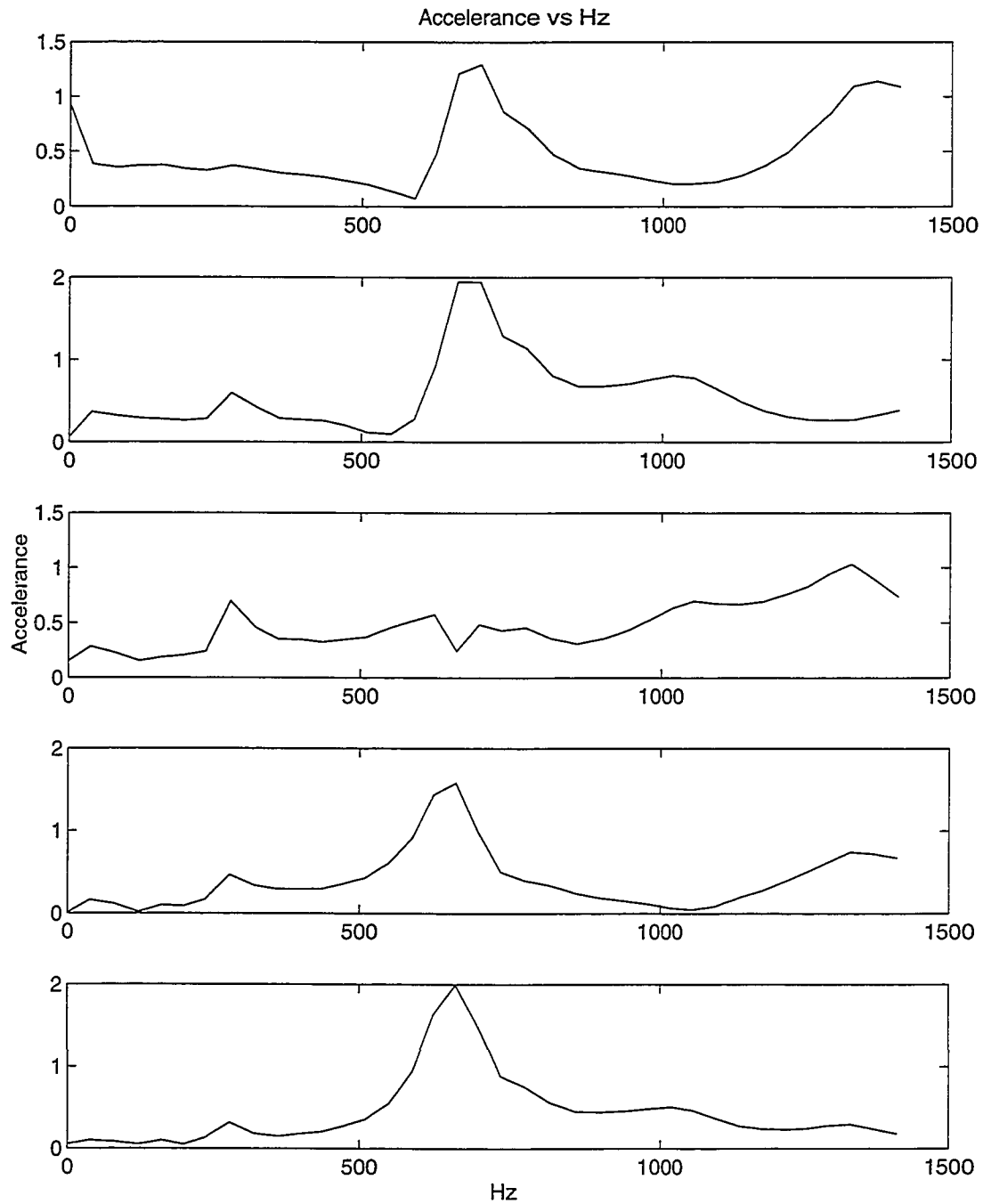
**Figure 5.4:** Accelerance vs Frequency (from top to bottom) at 6,12,18,24,30 cm, respectively, In Situ Femur #2 Without DVA
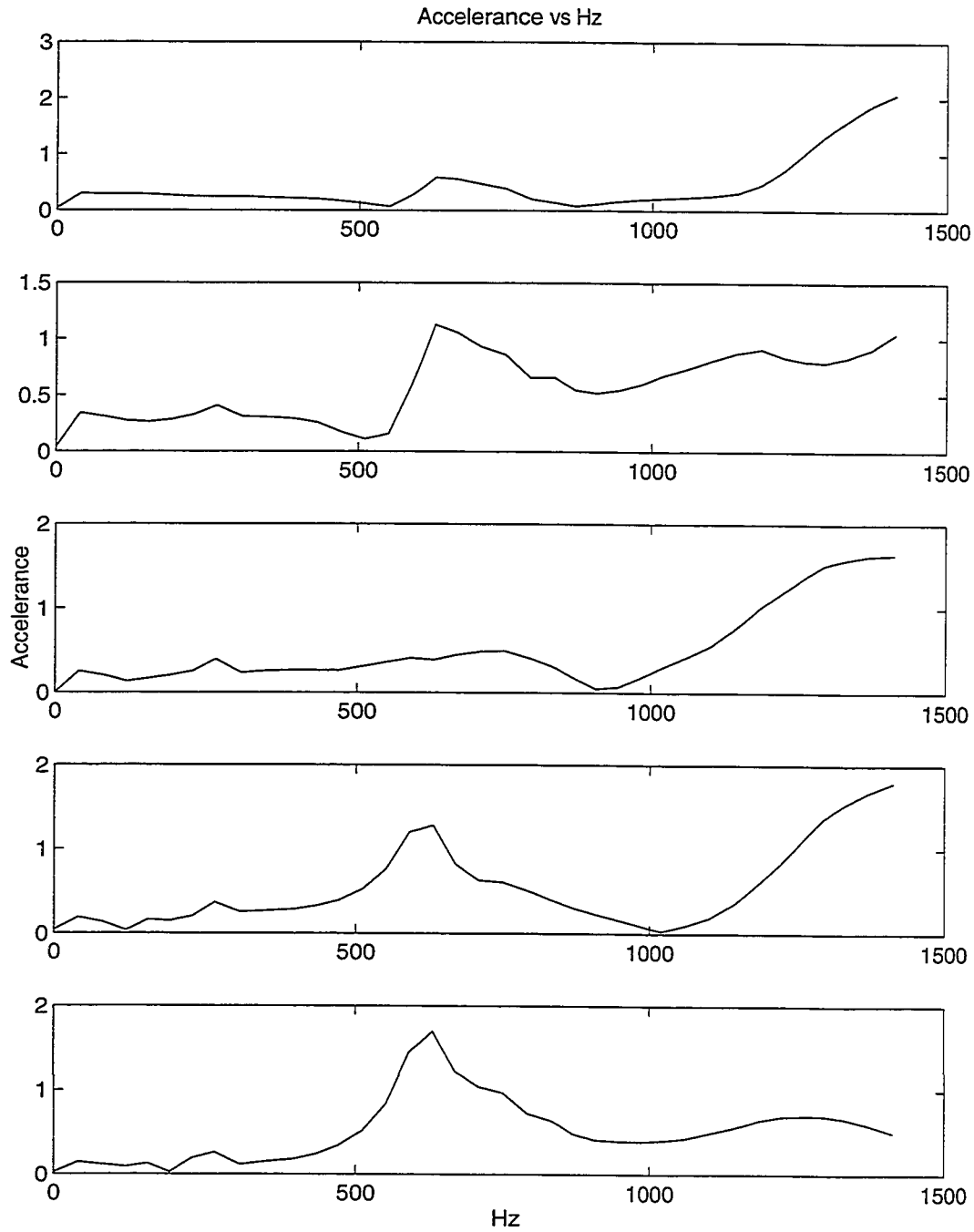
**Figure 5.5:** Accelerance vs Frequency (from top to bottom) at 6,12,18,24,30 cm, respectively, In Situ Femur #2 With DVA Mounted 9 cm Below Calcar
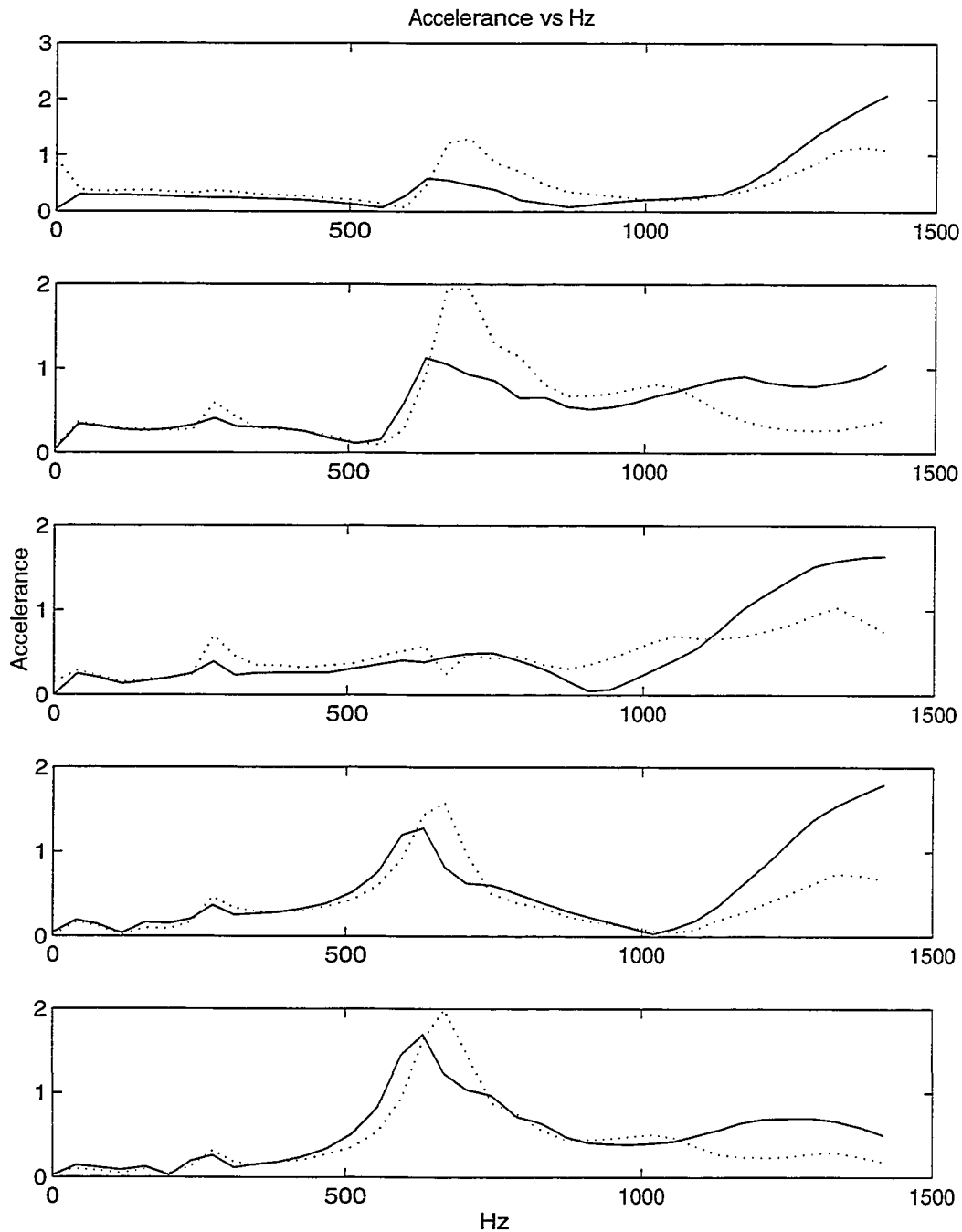
**Figure 5.6:** Accelerance vs Frequency (from top to bottom) at 6,12,18,24,30 cm, respectively, In Situ Femur #2 With (Solid Lines) and Without DVA (Dotted Lines), for Comparison
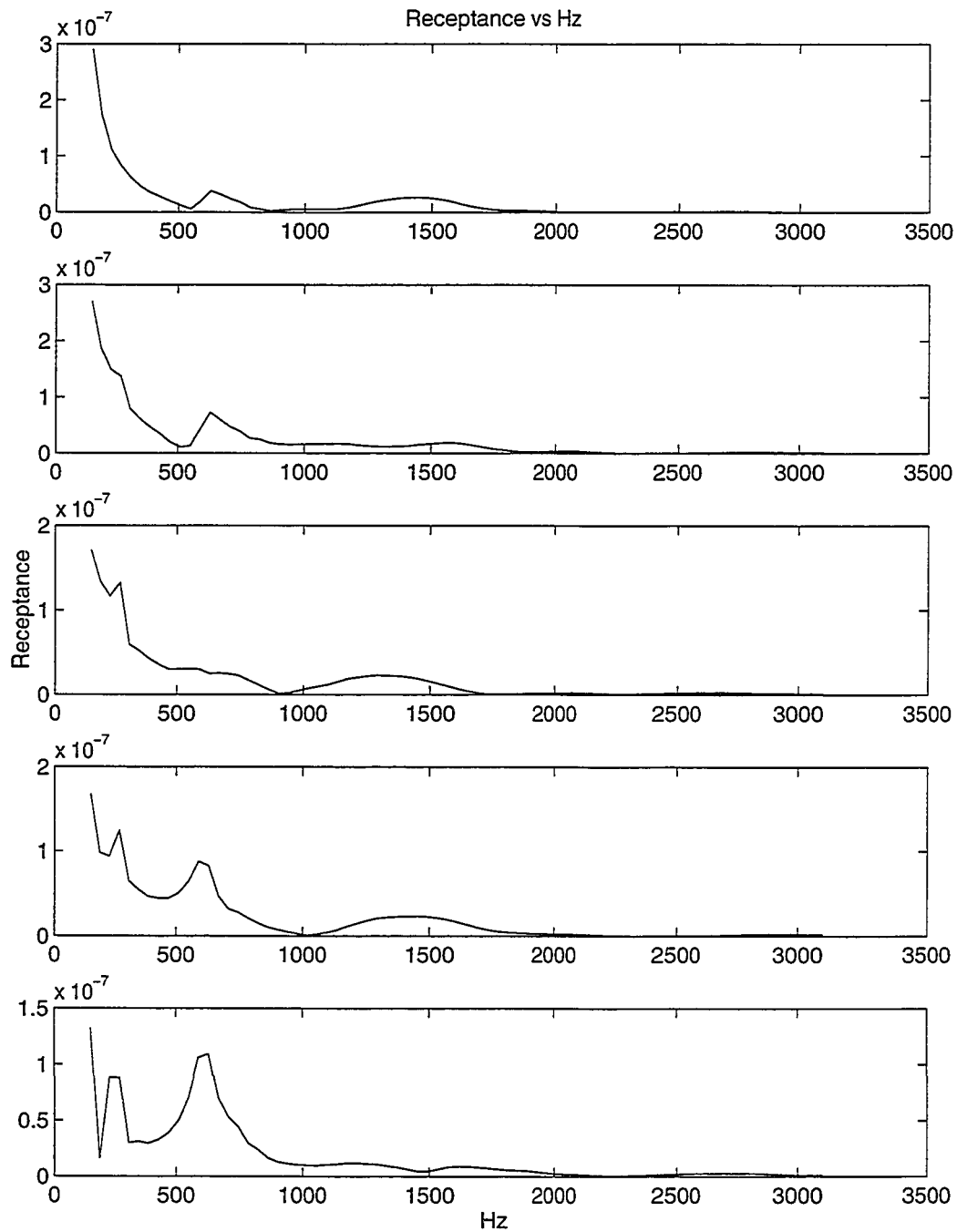
**Figure 5.7:** Receptance vs Frequency (from top to bottom) at 6,12,18,24,30 cm, respectively, In Situ Femur #2 With DVA Mounted 9 cm Below Calcar

almost any natural frequency in this neighborhood, with the possible exception of a narrow region around 500 Hz. In the second plot, Figure 5.9, the reaming process has progressed somewhat, and the peaks have shifted to the left slightly, but the 500 Hz dip remains in roughly the same place.

## 5.3 Testing of Excised Femur Without DVA

### 5.3.1 Subject to Free-Free Boundary Conditions

The plot of accelerance versus frequency when the excised femur is tested with free-free boundary conditions is seen in Figure 5.10. The primary peak occurs at roughly 700 Hz, in a very similar position as for the in situ case. A smaller peak occurs at
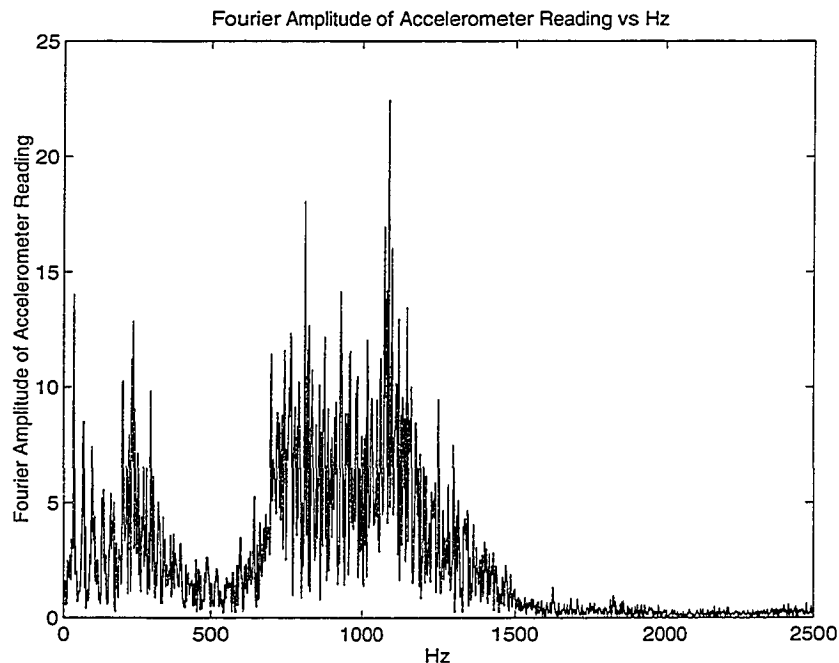


Figure 5.8: Fourier Amplitude of Accelerometer Reading when Femur Excited by Reamer, run 38

Fourier Amplitude of Accelerometer Reading vs Hz
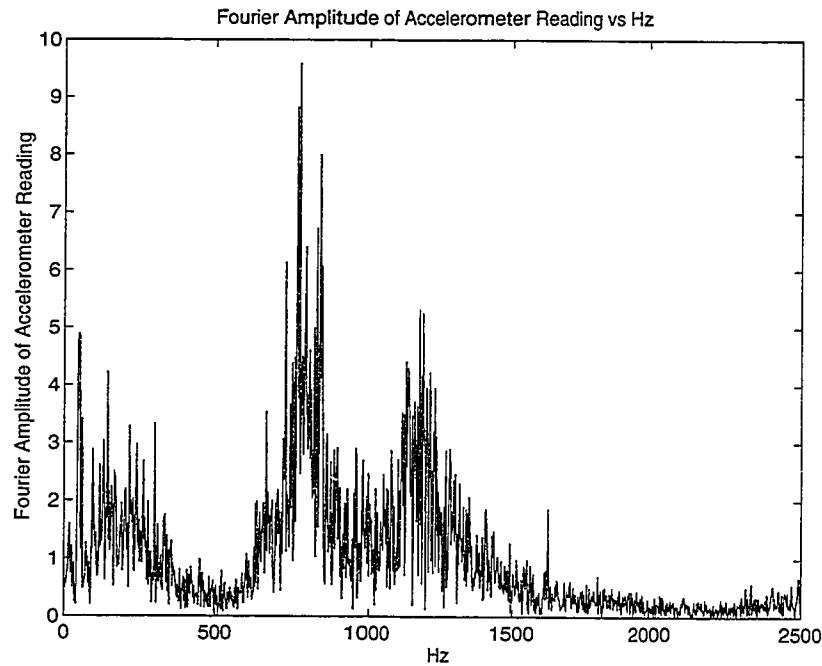
**Figure 5.9:** Fourier Amplitude of Accelerometer Reading when Femur Excited by Reamer, run 40

some points along the femur at approximately 250 Hz, again similar to the in situ case.

### 5.3.2 Subject to Simple-Free Boundary Conditions

When subjected to simple-free boundary conditions, the same femur has its most significant response at essentially the same frequency as the in situ and free-free cases. As in the other cases, a smaller peak also occurs around 250 Hz.

**Figure 5.10:** Accelerance vs Frequency (from top to bottom) at 6,12,18,24,30,36 cm, respectively, Excised Femur Subject to Free-Free Boundary Conditions, Without DVA

**Figure 5.11:** Accelerance vs Frequency (from top to bottom) at 6,12,18,24,30,36 cm, respectively, Excised Femur Subject to Simple-Free Boundary Conditions, Without DVA

## 5.4 Testing of Excised Femur With DVA

The last case examined is the case of the same femur subject to simple-free boundary conditions, with the same DVA attached in the same location as the in situ case. The results are shown in Figures 5.12 and 5.13.

In comparing the results without and with a DVA, the most significant point is that the absorber almost completely eliminates the 700 Hz peak at every measured point along the femur. It is also important to note that the response with the vibration absorber remains less than the response without it, even for the higher frequencies where the in situ case showed larger response with the damper (see Figure 5.6). This would indicate that nonlinearities in the in situ boundary conditions caused this phenomenon.

**Figure 5.12:** Accelerance vs Frequency (from top to bottom) at 6,12,18,24,30,36 cm, respectively, Excised Femur Subject to Simple-Free Boundary Conditions, With DVA Mounted 9 cm Below Calcar

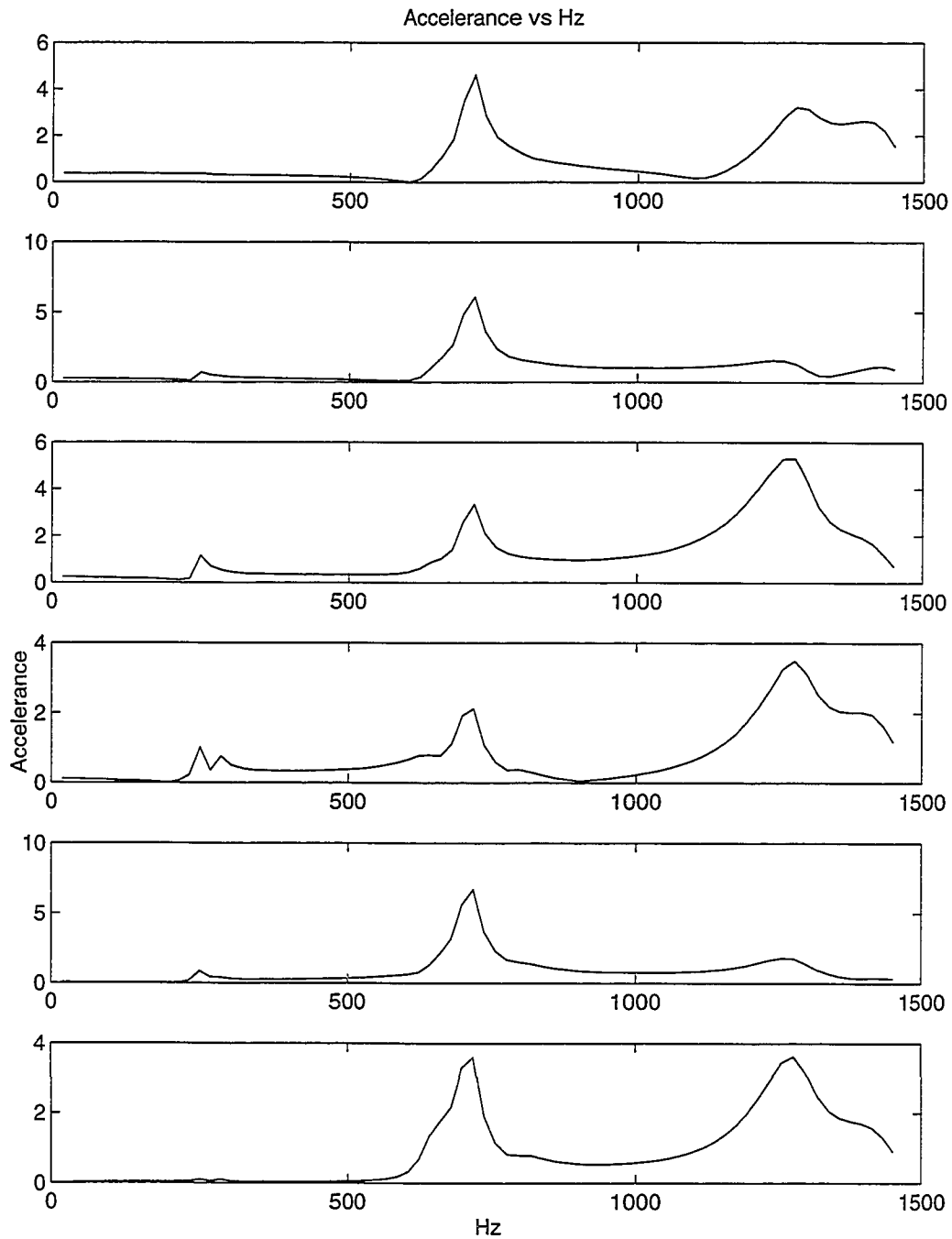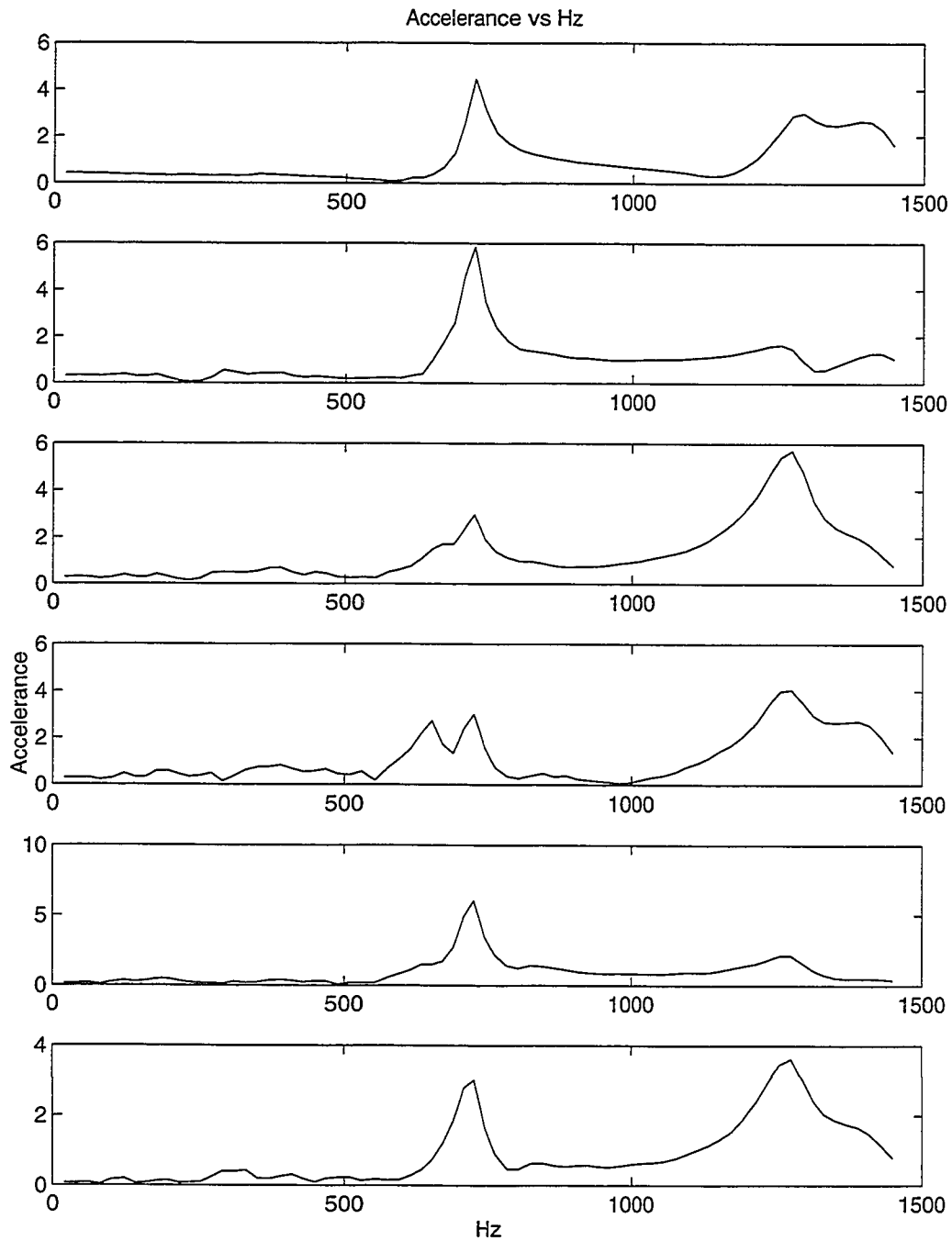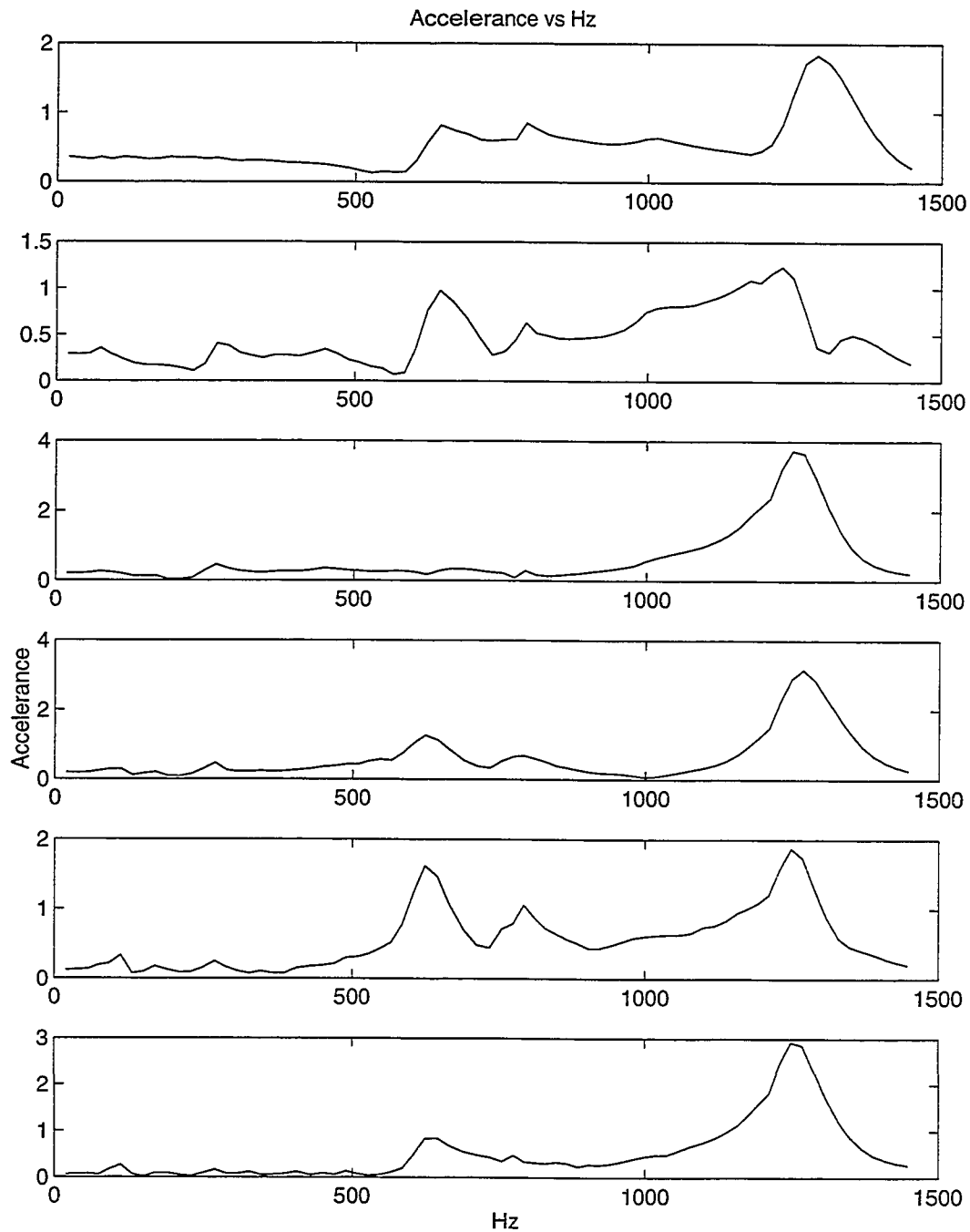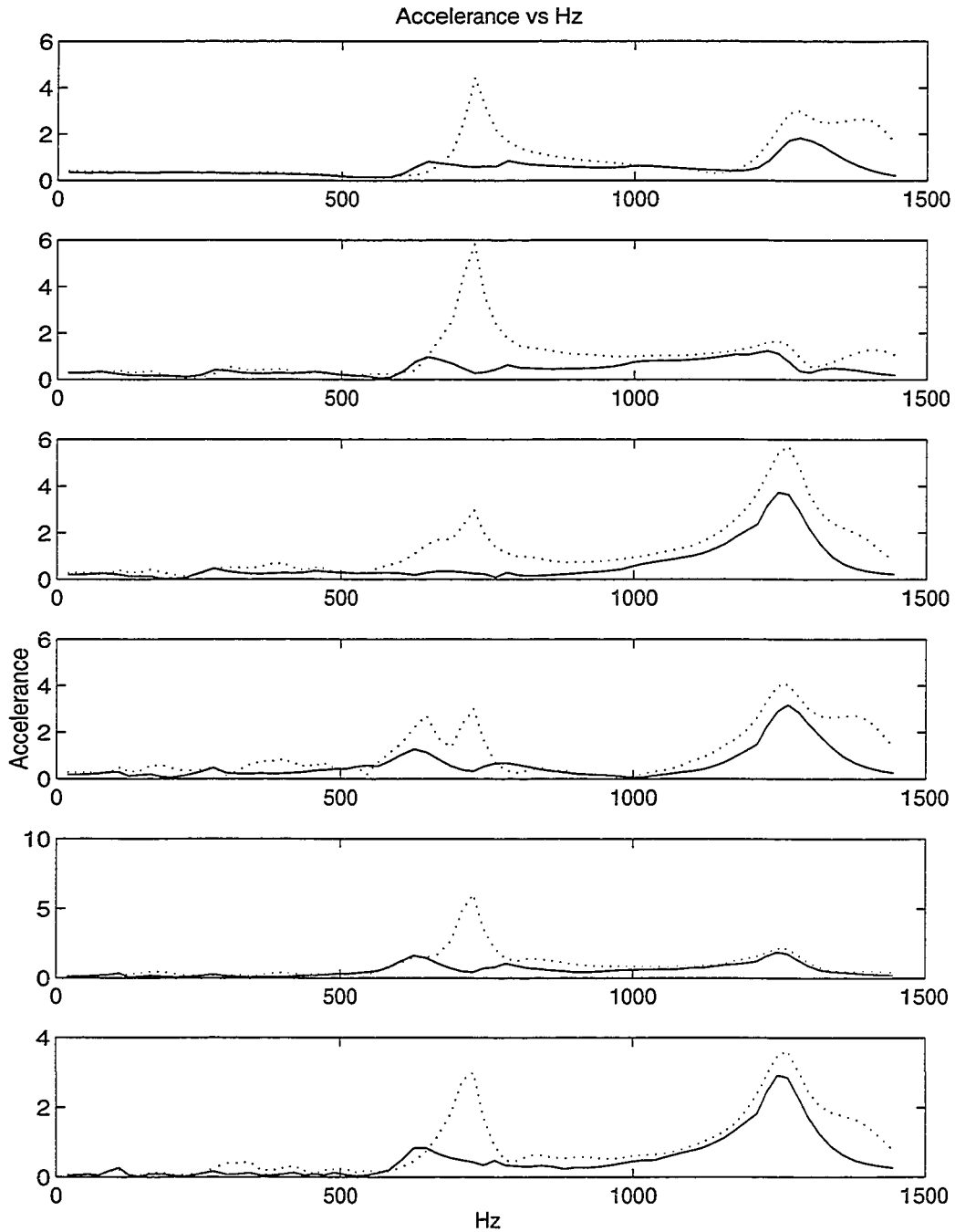**Figure 5.13:** Accelerance vs Frequency (from top to bottom) at 6,12,18,24,30,36 cm, respectively, Excised Femur Subject to Simple-Free Boundary Conditions, With (Solid Lines) and Without DVA (Dotted Lines), for Comparison

# Chapter 6

# Conclusions and Recommendations

Based on these results, several conclusions can be reached. Primarily, it does seem possible to significantly alter the vibrations of the femur by the attachment of a vibration absorber. This absorber will need to be tuned appropriately, and the degree to which this can be readily done for patients in the operating room needs additional investigation. Some standardization of the surgical technique appears to be necessary. One major example of this is removal of the femoral head in relation to the reaming process. Additionally, the boundary conditions during surgery need to be better understood, so that this vibration absorber can be properly tuned. Perhaps the surgical technique could be altered so that the boundary conditions will be more reproducible. This would allow both greater accuracy in analysis of a vibration absorber, as well as more effective application of such an absorber. As these issues are addressed a vibration absorber will have increasing usefulness in the reaming operation during hip replacement surgery. One encouraging development is that it does not appear that the cost of manufacturing a suitable vibration absorber is prohibitive. The materials used were not costly and are readily machined to the necessary configuration, once that is determined.

An interesting result which is unexpected is the similarity of the response of the femur, whether subject to free-free or simple-free boundary conditions.This is somewhat puzzling as beam theory would indicate that the natural frequencies should be different, but the fact that the same natural frequencies are important in all cases

may simplify the development of a clinically useful vibration absorber, as it could become less critical to perfectly understand the boundary conditions.

Future research in this area should focus on the boundary conditions and ways in which changing or standardizing these boundary conditions could make a vibration absorber more effective. Also, further work should be done to investigate making use of the region around 500 Hz where the reamer does not appear to excite the femur significantly. Perhaps part of the strategy in applying the DVA could be to shift the natural frequency to this neighborhood.

# Bibliography

[1] *Dorland's Illustrated Medical Dictionary, Twenty-Fifth Edition*, W. B. Saunders Company, 1974.

[2] M. Lalanne and P. Berthier and J. Der Hagopian, *Mechanical Vibrations for Engineers, (Trans. by F.C. Nelson)*, John Wiley and Sons, 1983.

[3] N. Eftekhar, *Total Hip Arthroplasty, Volume I*, Mosby-Year Book, 1993.

[4] S. Stulberg, B. Stulberg, R. Wixson, "The Rationale, Design Characteristics, and Preliminary Results of a Primary Custom Total Hip Prosthesis," *Clinical Orthopedics and Related Research*, **249**, 79-96, 1989.

[5] H. Amstutz, W. Luetzow, J. Moreland "Revision of femoral Component: Cemented and Cementless," *Hip Arthroplasty*, ed. H. Amstutz, 829-854, 1991.

[6] J. Charnley, *Low Friction Arthroplasty of the Hip, Theory and Practice*, Springer-Verlag, 1979.

[7] N. Eftekhar, *Total Hip Arthroplasty, Volume II*, Mosby-Year Book, 1993.

[8] C. Engh and J. Bobyn, *Biological Fixation in Total Hip Arthroplasty*, SLACK Incorporated, 1985.

[9] P. Walker and D. Robertson, "Design and Fabrication of Cementless Hip Stems" *Clinical Orthopedics and Related Research*, **235**, 25-34, 1988.

[10] P. Sandborn, S. Cook, W. Spires and M. Kester, "Tissue Response to Porous-coated Implants Lacking Initial Bone Apposition" *The Journal of Arthroplasty*, **337**, 337-346, 1988.

[11] W. Bargar, "Shape the Implant to the Patient, A Rationale for the Use of Custom-Fit Cementless Total Hip Implants," *Clinical Orthopedics and Related Research*, **249**, 73-78, 1989.

[12] D. Robertson, P. Walker, S. Hirano, X. Zhou, J. Granholm and R. Poss, "Improving the Fit of Press-Fit Hip Stems" *Clinical Orthopedics and Related Research*, **228**, 134-140, 1988.

[13] W. Capella, "Fit the Patient to the Prosthesis, An Argument Against the Routine Use of Custom Hip Implants," *Clinical Orthopedics and Related Research*, **249**, 56-59, 1989.

[14] M. Spector, S. Shortkroff, H. Hsu, N. Lane, C. Sledge, T. Thornhill "Tissue Changes Around Loose Prostheses, A Canine Model to Investigate the Effects of an Antiinflammatory Agent," *Clinical Orthopedics and Related Research*, **261**, 140-152, 1990.

[15] L. Dorr, R. Bloebaum, J. Emmanual, R, Meldrum, "Histologic, Biochemical and Ion Analysis of Tissue and Fluids Retrieved During Total Hip Arthroplasty," *Clinical Orthopedics and Related Research*, **261**, 82-95, 1990.

[16] R. Huiskes, "The Various Stress Patterns of Press-Fit, Ingrown, and Cemented Femoral Stems," *Clinical Orthopedics and Related Research*, **261**, 27-38, 1990.

[17] F. Haste, "Experimental Vibrational Investigation of the Relation Between Tool Chatter and Accuracy of the Reaming Process in Cementless Total Hip Surgery of the Human Femur" Master's Thesis, University of Kansas, 1994.

[18] F. Haste, "Dynamic Chatter During Femoral Reaming: Experimental Characterization of Natural Modes and Frequencies," Unpublished, 1993.

[19] T. Harrigan, "Proposal to the Whitaker Foundation for the Transfer of the Grant Entitled 'High Precision Preparation of Bone for Uncemented Prosthesis Fixation,' " University of Texas Health Science Center memorandum to the Whitaker Foundation, 1993.

[20] A. Thomas, D. Luo, J. Dunn, "Response of Human femur to Mechanical Vibration" *Journal of Biomedical Engineering*, **13**, 58-60, 1991.

[21] L. Meirovitch, *Analytical Methods in Vibrations*, The Macmillan Company, 1967.

[22] D. Young and R. Felgar, *Tables of Characteristic Functions Representing Normal Modes of Vibration of a Beam, University of Texas Publication Number 4913*, The University of Texas, 1949.

[23] S. Cowin, ed. *Bone Mechanics*, CRC Press, Inc., 1989.

[24] L. Meirovitch, *Elements in Vibration Analysis, Second Edition*, McGraw-Hill, 1986.

[25] D. Hartog, *Mechanical Vibrations*, Fourth Edition, McGraw-Hill, 1956.

[26] E.C. Pestel and F. A. Leckie, *Matrix Methods in Elastomechanics*, McGraw-Hill, 1963.

[27] K. Seto, "Vibration Control in Multi-Degree-of-Freedom Systems by Dynamic Absorbers (Report 2: On the Design of the Dynamic Absorbers Using the Transfer Matrix)," *Vibration Control and Active Vibration Suppression, DE-Vol 4,* ASME Press, 1987.

# Appendix A

# Source Code and Input Files for Beam Program

## A.1 Program to Calculate Frequency Response of Simple-Free Beam

```
program simp_res
implicit none
integer N,i,e_type(10),end_cond,Q
double precision E_b(10),Rho_b(10),S_b(10),I_b(10),L_b(10)
double precision M_att(10)
double precision M_s(10),I_s(10),K_s(10),R_s(10),zeta(10)
double precision w,winit,wstop,wincr
double precision A(8,8), T(8,8),T1(8,8)
double precision sub(4,4),bouncon(4),forc_ang(4)
double precision Yfree_i,Yfree_r,Ymag

open(1,file='full.out')

write(*,*)"enter # elements"
read(*,*) N

do 50 i=1,N
write(*,*)"Type of element",i
write(*,*)"1 is beam, 2 is attached mass,
$3 is suspended element"
10    read(*,*)e_type(i)
50    continue

do 500 i=1,N
if (e_type(i).eq.1) goto 100
if (e_type(i).eq.2) goto 200
if (e_type(i).eq.3) goto 300
```

```
100     write(*,*)"beam element",i," Young's Modulus"
        read(*,*) E_b(i)
        write(*,*)"beam element",i," Mass Density"
        read(*,*) Rho_b(i)
        write(*,*)"beam element",i," Cross Sectional Area"
        read(*,*) S_b(i)
        write(*,*)"beam element",i," Mom of Inertia"
        read(*,*) I_b(i)
        write(*,*)"beam element",i," Length"
        read(*,*) L_b(i)
        goto 450

200     write(*,*)"attached mass"
        read(*,*) M_att(i)
        goto 450

300     write(*,*)"susp element",i," mass"
        read(*,*) M_s(i)
        write(*,*)"susp element",i," Rotary Inertia"
        read(*,*) I_s(i)
        write(*,*)"susp element",i," stiffness"
        read(*,*) K_s(i)
        write(*,*)"susp element",i," rotary stiffness"
        read(*,*) R_s(i)
        write(*,*)"susp element",i," value for zeta (damping)"
        read(*,*) zeta(i)
        goto 450

450     continue
500     continue

* Enter end conditions
        write(*,*)"System end conditions, left-right:"
        write(*,*)"1:C-C  2:C-F  3:C-S  4:F-F  5:F-S  6:S-S  7:S-F"
```

```
        read(*,*) end_cond
*Sweep through frequencies and find response

        write(*,*)"Initial frequency of sweep in rad/s (must be >0)"
        read(*,*)winit
        write(*,*)"Final frequency of sweep in rad/s"
        read(*,*)wstop
        write(*,*)"Increment frequency of sweep in rad/s"
        read(*,*)wincr

        do 1000 w=winit,wstop,wincr


            do 600 Q=1,N

        if (e_type(Q).eq.1) call beamxfn(Q,E_b,S_b,L_b,I_b,Rho_b,w,A)
        if (e_type(Q).eq.2) call attxfn(Q,M_att,w,A)
        if (e_type(Q).eq.3) call suspxfn(Q,K_s,M_s,zeta,w,A)


* call subroutine to set matrix T equal to matrix A, if Q=1
            if(Q.eq.1) call set_eq(A,T)

* else call subroutine to premultiply matrix T by matrix A,
* return prod in T1
            if(Q.ne.1) then
            call matmult(A,T,T1)
            call set_eq(T1,T)
            end if

 600        continue


* form sub matrix for simple-free beam
        sub(1,1)=T(1,1)
```

```
        sub(1,2)=T(1,3)
        sub(1,3)=T(1,5)
        sub(1,4)=T(1,7)
        sub(2,1)=T(2,1)
        sub(2,2)=T(2,3)
        sub(2,3)=T(2,5)
        sub(2,4)=T(2,7)
        sub(3,1)=T(5,1)
        sub(3,2)=T(5,3)
        sub(3,3)=T(5,5)
        sub(3,4)=T(5,7)
        sub(4,1)=T(6,1)
        sub(4,2)=T(6,3)
        sub(4,3)=T(6,5)
        sub(4,4)=T(6,7)


* form free end boundary conditions,
* real force of magnitude 1 is bouncon(3)
*       bouncon(1)=imaginary force component,
* bouncon(3)=real force comp
*       bouncon(2)=imaginary moment component,
* bouncon(4)=real moment comp
        bouncon(1)=0.D0
        bouncon(2)=0.D0
        bouncon(3)=1.D0
        bouncon(4)=0.D0

        call DLSLRG(4,sub,4,bouncon,1,forc_ang)

* forc_ang is vector containing force and
* angle at simply-supported end
* for simple-free beam
* force_ang(1)=imag force comp at S end,
* force_ang(3)=real force comp at S end
* force_ang(2)=imag angle comp at S end,
```

```
* force_ang(4)=real angle comp at S end


        Yfree_i=T(4,1)*forc_ang(1)+T(4,3)*forc_ang(2)+
     $T(4,5)*forc_ang(3)+T(4,7)*forc_ang(4)


        Yfree_i=T(4,1)*forc_ang(1)+T(4,3)*forc_ang(2)+
     $T(4,5)*forc_ang(3)+T(4,7)*forc_ang(4)


        Yfree_r=T(8,1)*forc_ang(1)+T(8,3)*forc_ang(2)+
     $T(8,5)*forc_ang(3)+T(8,7)*forc_ang(4)


        Ymag=dsqrt((Yfree_i**2.D0)+(Yfree_r**2.D0))


        write(1,1100)w,Ymag,Yfree_i,Yfree_r
        write(1,*)

1000    continue
1100    format(1X,4(E14.6,2X))


        end


**************************************

        subroutine set_eq(IN,OUT)
        implicit none
        double precision IN(8,8), OUT(8,8)
        integer i,j
        do 50 i=1,8
        do 45 j=1,8
        OUT(i,j)=IN(i,j)
45      continue
50      continue

        end
```

```
***************************************

        subroutine idenmat(ANY)
        implicit none
        double precision ANY(8,8)
        integer i,j,k

        do 30 i=1,8
        do 20 j=1,8
        ANY(i,j)=0.D0
20      continue
30      continue

        do 50 k=1,8
        ANY(k,k)=1.D0
50      continue
        end


***************************************

* subroutine to premultiply matrix T by matrix A,return prod in T1
        subroutine matmult(A,T,T1)
        implicit none
        double precision A(8,8), T(8,8), T1(8,8)
        double precision part1, part2, part3, part4
        double precision part5, part6, part7, part8
        integer f,g

        do 50 f=1,8
        do 45 g=1,8

        part1=A(f,1)*T(1,g)
        part2=A(f,2)*T(2,g)
        part3=A(f,3)*T(3,g)
        part4=A(f,4)*T(4,g)
```

```
        part5=A(f,5)*T(5,g)
        part6=A(f,6)*T(6,g)
        part7=A(f,7)*T(7,g)
        part8=A(f,8)*T(8,g)


        T1(f,g)=part1+part2+part3+part4+part5+part6+part7+part8

45      continue
50      continue


        end
```

**********************************************

```
        subroutine beamxfn(Q,E_b,S_b,L_b,I_b,Rho_b,w,A)
        implicit none
        integer Q,j,k
        double precision E_b(10),Rho_b(10),S_b(10),I_b(10),L_b(10)
        double precision w,w2,A(8,8)
        double precision B2,B,B_1_4,B_L,EI

        w2=w**2.D0

        B2=w2*S_b(Q)*Rho_b(Q)/(I_b(Q)*E_b(Q))
        B=dsqrt(B2)
        B_1_4=dsqrt(dsqrt(B2))
        B_L=B_1_4*L_b(Q)
        EI=E_b(Q)*I_b(Q)

        A(1,1)=(dcosh(B_L)+dcos(B_L))/2.D0
        A(1,2)=-B_1_4*(dsinh(B_L)-dsin(B_L))/2.D0
        A(1,3)=EI*B*(dcosh(B_L)-dcos(B_L))/2.D0
        A(1,4)=-EI*B*B_1_4*(dsinh(B_L)+dsin(B_L))/2.D0

        A(2,1)=-(dsinh(B_L)+dsin(B_L))/(2.0*B_1_4)
```

```
      A(2,2)=A(1,1)
      A(2,3)=-EI*B_1_4*(dsinh(B_L)-dsin(B_L))/2.D0
      A(2,4)=A(1,3)

      A(3,1)=(dcosh(B_L)-dcos(B_L))/(2.D0*EI*B)
      A(3,2)=-(dsinh(B_L)+dsin(B_L))/(2.D0*EI*B_1_4)
      A(3,3)=A(1,1)
      A(3,4)=-B_1_4*(dsinh(B_L)-dsin(B_L))/2.D0

      A(4,1)=-(dsinh(B_L)-dsin(B_L))/(2.D0*EI*B*B_1_4)
      A(4,2)=A(3,1)
      A(4,3)=A(2,1)
      A(4,4)=A(1,1)

      do 100 j=5,8
      do 50 k=1,4
      A(j,k)=0.D0
50    continue
100   continue

      do 200 j=1,4
      do 150 k=5,8
      A(j,k)=0.D0
150   continue
200   continue

      do 300 j=1,4
      do 250 k=1,4
      A(j+4,k+4)=A(j,k)
250   continue
300   continue

      end
```

*******************************

67

```fortran
      subroutine attxfn(Q,M_att,w,A)
      implicit none
      integer Q
      double precision M_att(10),w,A(8,8)

      call idenmat(A)

      A(1,4)=-(M_att(Q))*(w**2.D0)
      A(5,8)=A(1,4)

      end

********************************

      subroutine suspxfn(Q,K2,M2,zeta,w,A)
      implicit none
      integer Q
      double precision A(8,8), K2(10), M2(10),w
      double precision omd,zeta(10),Nr,Ni,denom
      double precision denom1, denom2, denom3

      call idenmat(A)

      omd=dsqrt((K2(Q)/M2(Q)))

      Nr=(omd**2.D0)*((omd**2.D0)-(w**2.D0))+
     $((2.D0*zeta(Q)*omd*w)**2.D0)
      Ni=2.D0*zeta(Q)*omd*(w**3.D0)
      denom1=((omd**2.D0)-(w**2.D0))**2.D0
      denom2=(2.D0*zeta(Q)*omd*w)**2.D0
      denom3=M2(Q)*(w**2.D0)
      denom=-1.D0*(denom1+denom2)/denom3

      A(5,8)=Nr/denom
```

```
        A(5,4)=Ni/denom
        A(1,8)=-1.D0*Ni/denom
        A(1,4)=Nr/denom

        end


***************************************

        subroutine matprint(ANY)
        implicit none
        double precision ANY(8,8)
        integer i,j

        do 50 i=1,8
        write(*,100)(ANY(i,j),j=1,8)
 50     continue

        write(*,*)

100     format(1X,8(E8.2,1X))

        end
***************************************
```

## A.2   Sample Input File for Beam Without DVA

```
1
1
20.D9
2000.D0
1.4598D-04
1.0076D-08
0.48D0
7
100.D0
```

```
8100.D0
1.D0
```

## A.3   Sample Input File for Same Beam with DVA

```
3
1
2
3
20.D9
2000.D0
1.4598D-04
1.0076D-08
0.48D0
0.0171D0
0.0036D0
0.D0
1.1734D4
0.D0
0.D0
7
100.D0
8100.D0
1.D0
```